MycoKeys

MycoKeys 129: 43–80 (2026)
DOI: 10.3897/mycokeys.129.183371

Research Article

# Phylogeny, divergence time and historical biogeography of *Hyphoderma* (Hyphodermataceae, Polyporales): Introducing five new species from China

Wen Li[1,2], Haijiao Wang[2], Xiyan Wang[2], Xiuhe Liao[2], Kaisheng Wang[2], Wijesinghe Arachchige Subodini Nuwanthika[2], Changlin Zhao[1,2,3,4]

1 *Key Laboratory of Forest Disaster Warning and Control in Universities of Yunnan Province, Southwest Forestry University, Kunming 650224, China*
2 *College of Forestry, Southwest Forestry University, Kunming 650224, China*
3 *Department Microbial Drugs (MWIS), Helmholtz-Centre for Infection Research, 38124 Braunschweig, Germany*
4 *Modern Industry School of Edible-fungi, Southwest Forestry University, Kunming 650224, China*
*Corresponding author: Changlin Zhao (fungi@swfu.edu.cn; changlin.zhao@helmholtz-hzi.de)*

## Abstract

Species of *Hyphoderma* are important wood-inhabiting fungi and play a crucial role in forest ecosystems. Although species diversity within this genus has been increasingly documented in recent years, studies on its origin, evolutionary history, and biogeography remain limited. In this study, we compiled a global dataset of *Hyphoderma* sequences and reconstructed an updated phylogeny, divergence times, and biogeographic history of the genus *Hyphoderma* based on the internal transcribed spacer (ITS) region and nuclear large ribosomal subunit (nLSU) sequences. In addition, integrated morphological and phylogenetic analyses revealed five new *Hyphoderma* species. Molecular clock estimates indicated that the ancestor of *Hyphoderma* likely originated in the Cretaceous, with a mean stem age of 117.76 Mya (95% HPD = 92.38–147.74 Mya). Biogeographic reconstruction further suggested that Asia is the most probable ancestral area of *Hyphoderma* species. This study provides the first comprehensive inference of divergence times, biogeography, and speciation patterns within *Hyphoderma*.

**Key words:** Biogeographic patterns, molecular systematics, morphology, new taxa, reconstructing ancestral states, wood-decaying fungi

OPEN ACCESS

Academic editor: Yupeng Ge
Received: 23 December 2025
Accepted: 9 February 2026
Published: 19 February 2026

Citation: Li W, Wang H, Wang X, Liao X, Wang K, Subodini Nuwanthika WA, Zhao C (2026) Phylogeny, divergence time and historical biogeography of *Hyphoderma* (Hyphodermataceae, Polyporales): Introducing five new species from China. MycoKeys 129: 43–80. https://doi.org/10.3897/mycokeys.129.183371

Copyright: © Wen Li et al.
This is an open access article distributed under terms of the Creative Commons Attribution License (Attribution 4.0 International – CC BY 4.0).

## Introduction

The class Agaricomycetes is a diverse class of fungi within the Basidiomycota, encompassing mushrooms, bracket fungi, puff balls, and other fruiting body-forming species, which are found on all continents, including Antarctica, in habitats ranging from tropical rainforests to arctic and alpine ecosystems, and they have important ecological roles as decayers, mycorrhizal symbionts, and parasites of plants and fungi (Nagy et al. 2025). Saprotrophic Agaricomycetes are broadly categorized into wood decayers and litter decomposers, in which wood-decayer Agaricomycetes are further classified into white rot and brown rot based on the chemical and anatomical characteristics of the decayed wood (Floudas 2021). The genus *Hyphoderma* Wallr. (Hyphodermataceae,

Polyporales), typified by *H. setigerum* (Fr.) Donk, represents one of the most speciose and taxonomically challenging groups of wood-decaying fungi (Donk 1957; Nilsson et al. 2003; Kirk et al. 2008; Yurchenko and Wu 2015). Species of *Hyphoderma* typically produce resupinate to effuse-reflexed basidiomata with a ceraceous consistency, smooth to tuberculate or hydnoid hymenophores, a monomitic (rarely dimitic) hyphal system with clamp connections, with or without cystidia, suburniform to subcylindrical basidia, and smooth, thin-walled, ellipsoid to subglobose basidiospores (Bernicchia and Gorjón 2010). Species in this genus are white rot fungi (Wu 1997; Floudas et al. 2012; Guan et al. 2021; Duan et al. 2023; Yang et al. 2023). Currently, 217 specific and infraspecific names are recorded in Index Fungorum (accessed 7 February 2026), of which 125 are accepted worldwide, and 41 species are accepted in China (Nakasone 2008; Wu et al. 2010; Martín et al. 2018; Ma et al. 2021; Yang et al. 2023; Su et al. 2024; Li et al. 2025).

The traditionally circumscribed *Hyphoderma* was shown to be polyphyletic, and 20 species were transferred to *Peniophorella* within the Hymenochaetales (Larsson 2007). Subsequent studies further examined the delimitation of *Hyphoderma* and related genera, revealing that eight *Peniophorella* species form a distinct, well-supported clade separate from *Hyphoderma* (Tellería et al. 2012; Justo et al. 2017). Molecular systematic analyses have since provided a family-level phylogenetic framework for the order Polyporales and demonstrated that Hyphodermataceae contains only a single genus, *Hyphoderma*. A recent identification key to Chinese *Hyphoderma* species was published by Guan et al. (2021). Furthermore, multi-marker phylogenetic analyses based on ITS, nLSU, mtSSU, *rpb*1, and *rpb*2 sequence data revealed that *Hyphoderma* comprises several well-supported clades (Yang et al. 2023, 2025b).

Wood-decay fungi, as a group of macrofungi, possess significant economic and ecological value beyond their taxonomic importance. Biogeographical studies that address the origin, diversification, and distribution patterns of organisms are essential at the genus level for wood-decay fungi (Savinova et al. 2019; He et al. 2024; Hyde et al. 2024; Zhao et al. 2025). Recent advances have substantially improved our understanding of species diversity and divergence times in fungi, including many genera within the Agaricomycetes (He et al. 2019; Varga et al. 2019; Wang et al. 2023; Cui et al. 2025). Currently, more than 10,000 macrofungi species have been described (Hawksworth and Lücking 2017; Niskanen et al. 2023; Hibbett et al. 2025). Elucidating their origins, reconstructing evolutionary histories, and clarifying geographical distributions provide a strong foundation for forest ecosystem research and management (He et al. 2024; Zhao et al. 2025). Although the origin, evolution, and biogeography of certain genera, such as *Porodaedalea* and *Laetiporus*, have been well studied (Song and Cui 2017; Zhao et al. 2025), comparable research remains limited for many other genera, including *Hyphoderma*.

This research continues our long-term investigation into the taxonomy, phylogeny, and fungal diversity of wood-decaying fungi (Dai 2012; Mao et al. 2023; Cho et al. 2023; Pagin-Cláudio and Gugliotta 2024). The study aims to characterize novel and rare fungi, refine phylogenetic relationships within *Hyphoderma*, and provide new insights into the divergence times and biogeographical history of the genus. It is based on an integrative approach combining morphology and molecular phylogenetics. In addition, five new *Hyphoderma* species were

discovered in Yunnan Province, China. This research expands the taxonomic framework of *Hyphoderma* through modern taxonomic approaches and enhances our understanding of fungal evolution and geography.

## Materials and methods

### Sample collection and herbarium specimen preparation

Fresh basidiomata of fungi growing on angiosperm branches were collected from Yunnan Province, China. The samples were photographed in situ, metadata were recorded (Rathnayaka et al. 2025), and fresh macroscopic details were documented following the guidelines provided by Dong et al. (2024). All photographs were stacked and merged using Helicon Focus Pro 7.7.5 software. Specimens were dried in an electric food dehydrator at 40 °C, then sealed and stored in envelope bags (Dong et al. 2024, 2025), and deposited in the herbarium of Southwest Forestry University (**SWFC**), Kunming, Yunnan Province, P.R. China.

### Morphological examinations

Macro-morphological descriptions were based on field notes and photographs captured in the field and laboratory. The descriptions followed Petersen (1996) for color terminology. Micro-morphological characters were obtained from dried specimens observed under a light microscope at 1000× oil immersion (Dong et al. 2024, 2025). Sections were mounted in 5% KOH, 1% Congo Red solution, and 1% phloxine B ($C_{20}H_2Br_4Cl_4Na_2O_5$). Other reagents, including Cotton Blue and Melzer's reagent, were also used to observe micromorphology following the methods of Wu et al. (2019, 2022). To show variation in spore sizes, 5% of measurements were excluded from each end of the range and are shown in parentheses. At least 30 basidiospores from each specimen were measured. Stalks were excluded from basidia measurements, and the hilar appendage was excluded from basidiospore measurements (Yuan and Zhao 2024). The following abbreviations were used: **KOH** = 5% potassium hydroxide aqueous solution; **CB** = Cotton Blue; **CB–** = acyanophilous; **CB+** = cyanophilous; **IKI** = Melzer's reagent; **IKI–** = both inamyloid and indextrinoid; **L** = mean spore length (arithmetic average of all spores); **W** = mean spore width (arithmetic average of all spores); **Q** = variation in the L/W ratios between the specimens studied; and **n** = a/b (number of spores (a) measured from a given number (b) of specimens).

### DNA extraction, PCR amplification, sequencing

The CTAB rapid fungal genome extraction kit DN14 (Aidlab Biotechnologies Co., Ltd., Beijing, China) was used to obtain genomic DNA from dried fungal specimens according to the manufacturer's instructions. The extracted DNA was maintained at −20 °C for long-term storage. Two molecular markers were investigated: the internal transcribed spacer (ITS) region and the nuclear large subunit ribosomal RNA (LSU) gene. PCR primers and conditions are shown in Table 1. PCR products were purified and sequenced at Kunming Tsingke Biological Technology Limited Company (Yunnan Province, China). All newly generated sequences were deposited in NCBI GenBank (Sayers et al. 2025) (Table 1).

**Table 1.** Taxa information and GenBank accession numbers used in this study [* indicates type materials; — indicates sequence unavailability].

| Species Name | Sample No. | GenBank Accession No. | | References | Country |
|---|---|---|---|---|---|
| | | ITS | nLSU | | |
| *Amylocorticium cebennense* | HHB-2808 | GU187505 | GU187561 | Wang et al. 2023 | USA |
| *Anomoloma myceliosum* | MJL-4413 | GU187500 | GU187559 | Wang et al. 2023 | USA |
| *Aroramyces gelatinosporus* | H4010 | – | DQ218524 | Wang et al. 2023 | USA |
| *Athelia arachnoidea* | CBS 418.72 | GU187504 | GU187557 | Wang et al. 2023 | Netherlands |
| *Auricularia heimuer* | Xiaoheimao | LT716074 | KY418890 | Wang et al. 2023 | China |
| *Boletopsis leucomelaena* | AFTOL-ID 1527 | DQ484064 | DQ154112 | Wang et al. 2023 | USA |
| *Calocera cornea* | AFTOL 438 | AY789083 | AY701526 | Wang et al. 2023 | USA |
| *Coltricia abieticola* | Cui 10321 | KX364785 | KX364804 | Wang et al. 2023 | China |
| *Coniferiporia qilianensis* | Dai 13320 | MT416471 | MT386051 | Wang et al. 2023 | China |
| *Coniophora arida* | FP104367 | GU187510 | GU187573 | Wang et al. 2023 | USA |
| *Corticium boreoroseum* | MG 42 | MW805842 | MW805816 | Wang et al. 2023 | Sweden |
| *Dacryopinax spathularia* | AFTOL 454 | AY854070 | AY701525 | Wang et al. 2023 | USA |
| *Diplomitoporus crustulinus* | FD-137 | KP135299 | KP135211 | Justo et al. 2017 | USA |
| *Echinodontium tinctorium* | AFTOL-ID 455 | AY854088 | AF393056 | Wang et al. 2023 | USA |
| *Fomitopsis ostreiformi* | Cui 18217 | OL621855 | OL621244 | Wang et al. 2023 | China |
| *F. subtropica* | Dai 18566 | OL621854 | OL621243 | Wang et al. 2023 | China |
| *Gomphidius roseus* | MB 95-038 | DQ534570 | DQ534669 | Wang et al. 2023 | Germany |
| *Heterobasidion annosum* | 06129/6 | KJ583211 | KJ583225 | Wang et al. 2023 | China |
| ***Hyphoderma alboarachnum**** | **CLZhao 30488** | **PV470563** | **—** | **Present study** | **China** |
| *H. amoenum* | USO 286622 | HE577030 | — | Tellería et al. 2012 | Canada |
| *H. asianum** | CLZhao 18091 | OR141726 | PP826262 | Yang et al. 2025b | China |
| *H. assimile* | CBS:125852 | MH863808 | MH875272 | Vu et al. 2019 | New Zealand |
| *H. australosetigerum** | MA-Fungi 92235 | MN963764 | | Boonmee et al. 2021 | Chile |
| *H. australosetigerum* | MA-Fungi 92240 | MN963760 | | Boonmee et al. 2021 | Chile |
| ***H. bambusinum**** | **CLZhao 29903** | **PV469674** | **PV819428** | **Present study** | **China** |
| *H. cinereofuscum** | CLZhao 30341 | PQ492371 | PQ511128 | Li et al. 2025 | China |
| *H. cinereofuscum* | CLZhao 30283 | PQ492372 | PQ511129 | Li et al. 2025 | China |
| *H. cremeoalbum* | NH 11538 (GB) | DQ677492 | DQ677492 | Larsson 2007 | Sweden |
| *H. cremeoalbum* | CLZhao 17007 | OM985716 | OM985753 | Duan et al. 2023 | China |
| *H. crystallinum** | CLZhao 9338 | MW917161 | MW913414 | Guan and Zhao 2021a | China |
| *H. crystallinum* | CLZhao 9374 | MW917162 | MW913415 | Guan and Zhao 2021a | China |
| *H. definitum* | NH 12266 (GB) | DQ677493 | DQ677493 | Larsson 2007 | China |
| *H. fissuratum* | CLZhao 6731 | MT791331 | — | Ma et al. 2021 | China |
| *H. fissuratum** | CLZhao 6726 | MT791330 | MT791334 | Ma et al. 2021 | China |
| *H. floccosum** | CLZhao 17129 | MW301683 | MW293733 | Guan and Zhao 2021b | China |
| *H. floccosum* | CLZhao 17215 | MW301687 | MW293735 | Guan and Zhao 2021b | China |
| ***H. fulgens*** | **CLZhao 30254** | **PV469670** | **PV819427** | **Present study** | **China** |
| ***H. fulgens*** | **CLZhao 36600** | **PV829546** | **PV810096** | **Present study** | **China** |
| ***H. fulgens**** | **CLZhao 37429** | **PV829544** | **PV810095** | **Present study** | **China** |
| ***H. fulgens*** | **CLZhao 39474** | **PV829547** | **PV810098** | **Present study** | **China** |
| *H. granuliferum* | 5273 | JN710545 | JN710545 | Yurchenko and Wu 2014a | Canada |
| ***H. grandineum**** | **CLZhao 30046** | **PV470561** | **PV819429** | **Present study** | **China** |
| ***H. grandineum*** | **CLZhao 43328** | **PV470562** | **PV819430** | **Present study** | **China** |
| *H.guangdongense** | CLZhao 12657 | PP235513 | PP235514 | Su et al. 2024 | China |
| *H. incrustatum* | KHL6685 | — | AY586668 | Yurchenko and Wu 2014a | Spain |
| ***H. laceratum*** | **CLZhao 34242** | **PV829552** | **PV810101** | **Present study** | **China** |
| ***H. laceratum*** | **CLZhao 34672** | **PV829553** | **PV810103** | **Present study** | **China** |
| ***H. laceratum*** | **CLZhao 34958** | **PV829556** | **PV810106** | **Present study** | **China** |
| ***H. laceratum*** | **CLZhao 34961** | **PV829557** | | **Present study** | **China** |
| *H. litschaueri* | NH 7603 (GB) | DQ677496 | DQ677496 | Larsson 2007 | Sweden |
| *H. litschaueri* | FP-101740-Sp | KP135295 | KP135219 | Floudas and Hibbett 2015 | USA |

| Species Name | Sample No. | GenBank Accession No. | | References | Country |
|---|---|---|---|---|---|
| | | ITS | nLSU | | |
| *H. macaronesicum* | MA:Fungi 90388 | KC984327 | – | Tellería et al. 2012 | USA |
| *H. macaronesicum* | TFC:Mic 15115 | HE577011 | – | Yurchenko and Wu 2014b | China |
| *H. marginatum** | CLZhao 3404 | OM985717 | OM985754 | Duan et al. 2023 | China |
| *H. medioburiense* | FD-335 | KP135298 | KP135220 | Floudas and Hibbett 2015 | China |
| *H. membranaceum** | CLZhao 5844 | MW917167 | MW913420 | Guan and Zhao 2021a | China |
| *H. membranaceum* | CLZhao 6971 | MW917168 | MW913421 | Guan and Zhao 2021a | China |
| *H. microporoides* | CLZhao 6857 | MW917169 | MW913422 | Guan and Zhao 2021a | China |
| *H. microporoides* | CLZhao 8695 | MW917170 | MW913423 | Guan and Zhao 2021a | China |
| *H. moniliforme** | Wu 0211-42 | KC928282 | – | Yurchenko and Wu 2015 | China |
| *H. moniliforme* | Wu 0211-46 | KC928284 | – | Yurchenko and Wu 2015 | China |
| *H. mopanshanense** | CLZhao 6498 | MT791329 | MT791333 | Ma et al. 2021 | China |
| *H. mopanshanense* | CLZhao 6449 | OM985720 | OM985759 | Duan et al. 2023 | China |
| *H. nemorale* | TNM F3931 | KJ885183 | KJ885184 | Yurchenko and Wu 2015 | China |
| *H. nemorale* | Wu 9508-14 | KC928280 | KC928281 | Yurchenko and Wu 2015 | China |
| *H. niveomarginatum** | CLZhao 25078 | OR141728 | OR506179 | Yang et al. 2023 | China |
| *H. nudicephalum* | Wu9307_29 | AJ534269 | – | Nilsson et al. 2003 | China |
| *H. nudicephalum* | CLZhao 17839 | OM985721 | OM985760 | Duan et al. 2023 | China |
| *H. obtusiforme* | KHL1464 | JN572909 | – | Yurchenko and Wu 2014b | Spain |
| *H. obtusiforme* | KHL11105 | JN572910 | – | Yurchenko and Wu 2014b | Spain |
| *H. obtusum* | JS17804 | – | AY586670 | Yurchenko and Wu 2014b | China |
| *H. occidentale* | KHL 8477 (GB) | DQ677499 | DQ677499 | Larsson 2007 | China |
| *H. paramacaronesicum** | MA:Fungi 87736 | KC984399 | – | Martín et al. 2018 | USA |
| *H. paramacaronesicum* | MA:Fungi 87737 | KC984405 | – | Martín et al. 2018 | China |
| *H. pinicola* | Wu 0108-32 | KJ885181 | KJ885182 | Yurchenko and Wu 2014b | China |
| *H. pinicola* | Wu 0108-36 | KC928278 | KC928279 | Yurchenko and Wu 2014b | China |
| *H. prosopidis* | ARIZ HHB 8479 | HE577029 | – | Yurchenko and Wu 2015 | China |
| *H. puerense** | CLZhao 9476 | MW443045 | – | Guan et al. 2021 | China |
| *H. puerense* | CLZhao 9583 | MW443046 | MW443051 | Guan et al. 2021 | China |
| *H. qujingense** | CLZhao 26018 | OR141729 | PP826263 | Yang et al. 2025b | China |
| *H. roseocremeum* | NH 10545 | | AY586672 | Yurchenko and Wu 2014a | Sweden |
| *H. setigerum* | FCUG 1200 | AJ534273 | – | Nilsson et al. 2003 | Sweden |
| *H. setigerum* | FCUG 1688 | AJ534272 | – | Nilsson et al. 2003 | Sweden |
| *H. sinense** | CLZhao 7963 | MW301679 | MW293730 | Guan and Zhao 2021b | China |
| *H. sinense* | CLZhao 17811 | MW301682 | MW293732 | Guan and Zhao 2021b | China |
| *H. sordidum* | CLZhao 27379 | OR141731 | – | Yang et al. 2023 | China |
| *H. sordidum** | CLZhao 27390 | OR141732 | OR506180 | Yang et al. 2023 | China |
| *H. subsetigerum* | HHB11620 | GQ409521 | – | Yurchenko and Wu 2014a | China |
| *H. tenuissimum** | CLZhao 7221 | MW443049 | MW443054 | Guan et al. 2021 | China |
| *H. tenuissimum* | CLZhao 16210 | MW443050 | MW443055 | Guan et al. 2021 | China |
| *H. transiens* | NH 12304 | DQ677504 | DQ677504 | Larsson 2007 | Sweden |
| *H. tropicum** | CLZhao 17308 | OM985727 | OM985768 | Duan et al. 2023 | China |
| *H. variolosum* | CBS:734.91 | MH862320 | MH873992 | Vu et al. 2019 | China |
| *H. variolosum* | CBS:735.91 | MH862321 | MH873993 | Vu et al. 2019 | China |
| *H. weishanense** | CLZhao 22403 | OR141727 | OR506181 | Yang et al. 2023 | China |
| *H. yunnanense* | CLZhao 8845 | OM985728 | OM985769 | Duan et al. 2023 | China |
| *Hyphodontia pachyspora* | LWZ 20170908-5 | MT319426 | MT319160 | Wang et al. 2023 | China |
| *Hymenochaete sphaericola* | LWZ20190808-2b | ON063656 | ON063855 | Wang et al. 2023 | China |
| *Jaapia argillacea* | CBS 252.74 | GU187524 | GU187581 | Wang et al. 2023 | Netherlands |
| *Laetisaria fuciformis* | CBS:182.49 | MH856485 | MH868023 | Vu et al. 2019 | Netherlands |
| *Leptosporomyces raunkiaerii* | HHB-7628 | GU187528 | GU187588 | Wang et al. 2023 | USA |
| *Lyomyces incanus* | CLZhao 22900 | OR094481 | OR449936 | Dong et al. 2024 | China |
| *Meripilus giganteus* | FP 135344 | KP135307 | KP135228 | Wang et al. 2023 | USA |
| *Neurospora crassa* | VB2 | HQ271348 | AF286411 | Wang et al. 2023 | India |
| *Nigrofomes sinomelanoporus* | Cui 5277 | MF629836 | MF629832 | Wang et al. 2023 | China |

| Species Name | Sample No. | GenBank Accession No. | | References | Country |
|---|---|---|---|---|---|
| | | ITS | nLSU | | |
| *Phanerochaete aculeata* | Wu 880701-2 | MZ422787 | GQ470636 | Wang et al. 2023 | China |
| *Phanerochaete mopanshanensis* | CLZhao 2357 * | OR096190 | OR461450 | Dong et al. 2024 | China |
| *Physisporinus longicystidius* | Cui 16630 | ON417177 | ON417227 | Wang et al. 2023 | China |
| *Polyporus squamosus* | Cui 10595 | KU189778 | KU189809 | Wang et al. 2023 | China |
| *Polyporus varius* | Cui 12249 | KU507581 | KU507583 | Wang et al. 2023 | China |
| *Peniophorella subpraetermissa* | LWZ 20190816-3b | ON063689 | ON063889 | Wang et al. 2023 | China |
| *Rigidoporus populinus* | LWZ 20190811-39a | ON063674 | ON063874 | Wang et al. 2023 | China |
| *Steccherinum weishanense* | CLZhao 24911 * | OR096207 | OR461456 | Dong et al. 2024 | China |
| *S. ochraceum* | KHL 11902 | JN710590 | JN710590 | Wang et al. 2023 | Sweden |
| *Thelephora ganbajun* | ZRL20151295 | LT716082 | KY418908 | Wang et al. 2023 | China |
| *Xylodon olivaceobubalinus* | CLZhao 25174 | OR167772 | OR449948 | Dong et al. 2024 | China |

## Phylogenetic analyses

ITS and nLSU sequences were aligned using MAFFT version 7 (Katoh et al. 2019) with the G-INS-i strategy. Single-gene alignments were manually adjusted using AliView version 1.27 (Larsson 2014; Caboň et al. 2019). The ITS and nLSU sequences were then combined using Mesquite version 3.51. The final sequence alignment, together with related information, was deposited in Figshare (DOI: https://doi.org/10.6084/m9.figshare.30939239). *Diplomitoporus crustulinus* (Bres.) Domanski was selected as the outgroup for phylogenetic analyses following Justo et al. (2017). Maximum parsimony (MP), maximum likelihood (ML), and Bayesian inference (BI) analyses were performed using the combined dataset. Phylogenetic analytical procedures followed Sun et al. (2022). MP analysis was conducted in PAUP* version 4.0b10 (Swofford 2002). All characters were equally weighted, and gaps were treated as missing data. Trees were inferred using a heuristic search with TBR branch swapping and 1,000 random sequence additions. Maxtrees were set to 5,000, branches of zero length were collapsed, and all most-parsimonious trees were saved.

Clade robustness was assessed using bootstrap (BT) analysis with 1,000 replicates (Felsenstein 1985; Guan et al. 2023). Descriptive tree statistics, including tree length (TL), consistency index (CI), retention index (RI), rescaled consistency index (RC), and homoplasy index (HI), were calculated for each most-parsimonious tree. ML analysis was conducted using RAxML-HPC2 through the CIPRES Science Gateway (www.phylo.org) (Miller et al. 2012). Branch support (BS) for ML analysis was estimated using 1,000 bootstrap replicates under the gamma model.

MrModeltest 2.3 (Nylander 2004) was used to determine the best-fit evolutionary model for each dataset. BI was performed in MrBayes 3.2.7a using the GTR+I+G model of DNA substitution with gamma-distributed rate variation across sites (Ronquist et al. 2012). Four Markov chains were run for two independent runs from random starting trees for four million generations for the ITS+nLSU dataset (Fig. 1), with trees and parameters sampled every 1,000 generations. The first one-fourth of all generations was discarded as burn-in. A majority-rule consensus tree was calculated from the remaining trees. Branches were considered significantly supported if they received a maximum likelihood bootstrap value (BS) ≥ 70%, a maximum parsimony bootstrap value (BT) ≥ 50%, or a Bayesian posterior probability (BPP) ≥ 0.95.

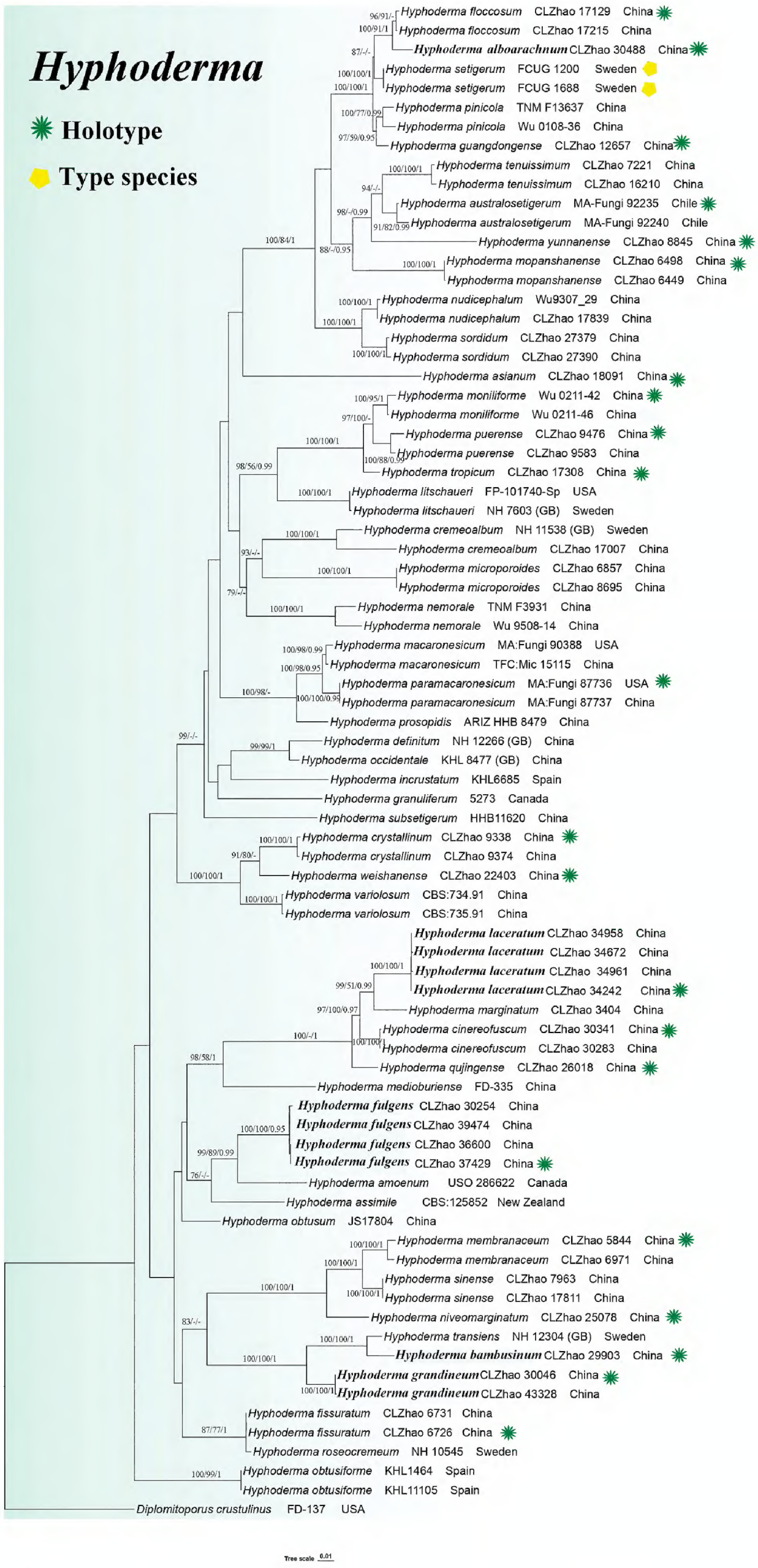
Hyphoderma
Holotype
Type species
Hyphoderma floccosum CLZhao 17129 China
Hyphoderma floccosum CLZhao 17215 China
Hyphoderma alboarachnum CLZhao 30488 China
Hyphoderma setigerum FCUG 1200 Sweden
Hyphoderma setigerum FCUG 1688 Sweden
Hyphoderma pinicola TNM F13637 China
Hyphoderma pinicola Wu 0108-36 China
Hyphoderma guangdongense CLZhao 12657 China
Hyphoderma tenuissimum CLZhao 7221 China
Hyphoderma tenuissimum CLZhao 16210 China
Hyphoderma australosetigerum MA-Fungi 92235 Chile
Hyphoderma australosetigerum MA-Fungi 92240 Chile
Hyphoderma yunnanense CLZhao 8845 China
Hyphoderma mopanshanense CLZhao 6498 China
Hyphoderma mopanshanense CLZhao 6449 China
Hyphoderma nudicephalum Wu9307_29 China
Hyphoderma nudicephalum CLZhao 17839 China
Hyphoderma sordidum CLZhao 27379 China
Hyphoderma sordidum CLZhao 27390 China
Hyphoderma asianum CLZhao 18091 China
Hyphoderma moniliforme Wu 0211-42 China
Hyphoderma moniliforme Wu 0211-46 China
Hyphoderma puerense CLZhao 9476 China
Hyphoderma puerense CLZhao 9583 China
Hyphoderma tropicum CLZhao 17308 China
Hyphoderma litschaueri FP-101740-Sp USA
Hyphoderma litschaueri NH 7603 (GB) Sweden
Hyphoderma cremeoalbum NH 11538 (GB) Sweden
Hyphoderma cremeoalbum CLZhao 17007 China
Hyphoderma microporoides CLZhao 6857 China
Hyphoderma microporoides CLZhao 8695 China
Hyphoderma nemorale TNM F3931 China
Hyphoderma nemorale Wu 9508-14 China
Hyphoderma macaronesicum MA:Fungi 90388 USA
Hyphoderma macaronesicum TFC:Mic 15115 China
Hyphoderma paramacaronesicum MA:Fungi 87736 USA
Hyphoderma paramacaronesicum MA:Fungi 87737 China
Hyphoderma prosopidis ARIZ HHB 8479 China
Hyphoderma definitum NH 12266 (GB) China
Hyphoderma occidentale KHL 8477 (GB) China
Hyphoderma incrustatum KHL6685 Spain
Hyphoderma granuliferum 5273 Canada
Hyphoderma subsetigerum HHB11620 China
Hyphoderma crystallinum CLZhao 9338 China
Hyphoderma crystallinum CLZhao 9374 China
Hyphoderma weishanense CLZhao 22403 China
Hyphoderma variolosum CBS:734.91 China
Hyphoderma variolosum CBS:735.91 China
Hyphoderma laceratum CLZhao 34958 China
Hyphoderma laceratum CLZhao 34672 China
Hyphoderma laceratum CLZhao 34961 China
Hyphoderma laceratum CLZhao 34242 China
Hyphoderma marginatum CLZhao 3404 China
Hyphoderma cinereofuscum CLZhao 30341 China
Hyphoderma cinereofuscum CLZhao 30283 China
Hyphoderma qujingense CLZhao 26018 China
Hyphoderma medioburiense FD-335 China
Hyphoderma fulgens CLZhao 30254 China
Hyphoderma fulgens CLZhao 39474 China
Hyphoderma fulgens CLZhao 36600 China
Hyphoderma fulgens CLZhao 37429 China
Hyphoderma amoenum USO 286622 Canada
Hyphoderma assimile CBS:125852 New Zealand
Hyphoderma obtusum JS17804 China
Hyphoderma membranaceum CLZhao 5844 China
Hyphoderma membranaceum CLZhao 6971 China
Hyphoderma sinense CLZhao 7963 China
Hyphoderma sinense CLZhao 17811 China
Hyphoderma niveomarginatum CLZhao 25078 China
Hyphoderma transiens NH 12304 (GB) Sweden
Hyphoderma bambusinum CLZhao 29903 China
Hyphoderma grandineum CLZhao 30046 China
Hyphoderma grandineum CLZhao 43328 China
Hyphoderma fissuratum CLZhao 6731 China
Hyphoderma fissuratum CLZhao 6726 China
Hyphoderma roseocremeum NH 10545 Sweden
Hyphoderma obtusiforme KHL1464 Spain
Hyphoderma obtusiforme KHL11105 Spain
Diplomitoporus crustulinus FD-137 USA
Tree scale 0.01

**Figure 1.** Phylogenetic tree generated from an ML analysis based on ITS+nLSU sequences. Branches are labeled with maximum likelihood bootstrap values equal to or higher than 70%, maximum parsimony bootstrap values equal to or higher than 50%, and Bayesian posterior probabilities equal to or higher than 0.95. Novel sequences are printed in bold.

## Estimation of divergence times

The divergence-time analysis followed methodologies outlined in previous studies (Wang et al. 2023; Cui et al. 2025). Using a secondary calibration approach, two independent analyses were conducted to estimate divergence times within *Hyphoderma*.

BEAST v2.6.0 was used to perform molecular clock analyses on the combined alignment derived from Table 1 (Sun et al. 2022; Wang et al. 2023; Cui et al. 2025). A lognormal relaxed molecular clock model and a Yule speciation prior were selected to estimate divergence times and their associated credibility intervals (Zhao and Wu 2017; Spirin et al. 2024). Two calibration points were applied. The first calibration used an offset age with a gamma distribution prior (scale = 20, shape = 1) for Basidiomycota at 400 Mya, based on the divergence between Ascomycota and Basidiomycota inferred from the fossil *Paleopyrenomycites devonicus*, discovered in Great Britain (Floudas et al. 2012). Trees were sampled every 1,000 generations over 200 million generations, with the first 10% discarded as burn-in. The resulting log files were examined for convergence using Tracer v1.5 (Wang et al. 2023).

Similarly, divergence times of species within *Hyphoderma* were estimated based on the results obtained above. This analysis included 48 samples representing a single genus of *Hyphoderma*, with *Meripilus giganteus* and *Physisporinus longicystidius* designated as outgroup taxa. Sequence data used in this analysis are provided in Table 2. These analyses were used to estimate the origin and biogeographical history of *Hyphoderma* species.

Divergence-time analyses were further conducted using BEAST v1.10.4 (He et al. 2024). XML input files were generated in BEAUti v1.10.4 by importing separate NEXUS files for each gene partition. Gene partitions were unlinked for substitution and molecular-clock models but linked for gene trees. Nucleotide substitution models were selected using jModelTest v2, with GTR+I+G applied to ITS and nrLSU. An uncorrelated lognormal relaxed clock model and a Yule speciation prior were used to assume a constant speciation rate per lineage. The prior distribution for the ucld.mean parameter was gamma-distributed (shape = 1.0, scale = 0.001, offset = 0.0) for all genes. Secondary calibrations were implemented using a normally distributed prior on the treeModel.rootHeight parameter (SD = 1), with mean values determined by fossil-based node calibrations. Four independent Markov chain Monte Carlo (MCMC) runs were performed, each consisting of 100,000,000 generations, with parameters sampled every 10,000 generations. Log files were assessed for convergence and mixing using Tracer v1.7.1 (Wang et al. 2023) (http://tree.bio.ed.ac.uk/software/tracer/) to confirm effective sample size (ESS) values exceeded 200. An ultrametric maximum clade credibility (MCC) tree, with mean node ages and 95% highest posterior density (HPD) intervals and per-clade posterior probabilities, was summarized using TreeAnnotator v1.10.4, applying a 25% burn-in and a posterior probability threshold of 0.8. Resulting trees were visualized using iTOL v5 (Wang et al. 2023; Zhao et al. 2023; Cui et al. 2025).

## Biogeographic analysis of *Hyphoderma*

Biogeographic analysis of the genus *Hyphoderma* was conducted using Reconstruct Ancestral State in Phylogenies (RASP) v4.2 with the Dispersal–Extinction–Cladogenesis (DEC) model, estimated through the BioGeoBEARS package

(Cui et al. 2025). Ancestral area reconstruction was performed using a posterior distribution of the aligned dataset 4, which was estimated in BEAST v2.6.5 with 10 million generations. The geographical distribution of *Hyphoderma* was divided into six regions: A) Asia, B) Europe, C) North America, D) South America, E) Africa, and F) Oceania.

**Table 2.** Morphological comparison of new species with similar taxa of the genus *Hyphoderma*.

| Species name | Basidiomata | Hyphal system | Cystidia | Basidiospores | References |
|---|---|---|---|---|---|
| *Hyphoderma alboarachnum* | Membranaceous, hymenial surface arachnoid. | Monomitic; generative hyphae with clamp connections, colorless, thin-walled. | Absent | Oblong-ellipsoid to cylindrical; 5–6 × 2–3 µm. | Present study |
| *H. asianum* | Ceraceous to membranaceous, hymenial surface smooth, floccose. | Monomitic; generative hyphae with clamp connections, colorless, thin-walled. | Moniliform; 20–50 × 4–6 µm. | Ellipsoid; 6.5–10 × 4–6 µm. | Yang et al. 2025b |
| *H. bambusinum* | Membranaceous, hymenial surface smooth. | Monomitic; generative hyphae with clamp connections, colorless, thin–to thick. | Tubular; 21.5–26.5 × 5–6.5 µm. | Ellipsoid; 4.5–6.5 × 3–4.5 µm. | Present study |
| *H. cinereofuscum* | Coriaceous, hymenial surface smooth. | Monomitic; generative hyphae with simple-septa, colorless, thin-walled. | 1) Tubular; 25.9–37.1 × 1.8–2.5 µm 2) Capitate; 12.5–15.5 × 6.2–7 µm. | Cylindrical; 9–11.5 × 4.5–5 µm. | Li et al. 2025 |
| *H. crystallinum* | Membranaceous, scattered nubby crystals. | Monomitic; generative hyphae with clamp connections, colorless, thin-walled. | 1) Tubular 32–51 × 5–10 µm. 2) Encrusted 14–46 × 4–11 µm. | Allantoid; 11–14.5 × 4–5.5 µm. | Guan and Zhao 2021a |
| *H. fissuratum* | Ceraceous, hymenial surface smooth. | monomitic, generative hyphae with clamp connections. | Absent | Cylindrical; 8.5–10.3 × 3–4 µm. | Ma et al. 2021 |
| *H. floccosum* | Ceraceous, hymenial surface farinaceous. | Monomitic; generative hyphae with simple-septa, colorless, thin-walled. | 1) septate 60–161 × 5.5–10 µm. 2) tubular 37.5–100 × 4–8.5 µm. | Ellipsoid to allantoid; 6–9.5 × 3–4.5 µm. | Guan and Zhao 2021b |
| *H. fulgens* | Membranaceous, hymenial surface smooth. | Monomitic; generative hyphae with simple-septa, colorless, thin-walled. | Clavate 37.1 × 5.5–7.5 µm. | Subcylindrical; 7.5–11.5 × 2.5–4 µm. | Present study |
| *H. grandineum* | Membranaceous, hymenial surface grandinioid. | Monomitic; generative hyphae with simple-septa, colorless, thin-walled. | Leptocystidia 29.5–33.5 × 4–5 µm. | Cylindrical;7–9 × 2.5–4 µm. | Present study |
| *H. laceratum* | Membranaceous, hymenial surface smooth. | Monomitic; generative hyphae with simple-septa, colorless, thin-walled. | 1) Clavate 27–29 × 6.5–8 µm. 2) Capitate 26–30 × 7.5–8.5 µm. | Subellipsoid; 6.5–9 × 3–4.5 µm. | Present study |
| *H. marginatum* | Membranaceous, hymenial surface smooth. | Monomitic; generative hyphae with simple-septa, colorless, thin-walled. | Cylindrical 30–48.5 × 7.5–11.5 µm. | Cylindrical; 9–10 × 3.5–4.5 µm. | Duan et al. 2023 |
| *H. membranaceum* | Membranaceous, hymenial surface tuberculate | Monomitic, generative hyphae with clamp thin-walled. | Moniliform; 28–60 × 6.5–10.5 µm. | Ellipsoid to cylindrical 11–13.5 × 4.5–5.5 µm. | Guan and Zhao 2021a |
| *H. microporoides* | Cottony hymenial surface smooth. | Monomitic, generative hyphae with clamp connections, colorless, thin-walled | Capitate; 18–51 × 4.5–7 µm. | Cylindrical to allantoid, 8.5–10 × 2.5–3.5 µm. | Guan and Zhao 2021a |
| *H. mopanshanense* | Ceraceous, hymenial surface porulose to pilose. | monomitic, generative hyphae bearing clamp connections | Fusiform; 86–171 × 10.5–13 µm | Cylindrical 7.8–9.7 × 2.6–3.3 µm. | Ma et al. 2021 |
| *H. niveomarginatum* | Ceraceous, hymenial surface smooth. | Monomitic, generative hyphae with clamp connections, colorless, thin-walled | Moniliform; 29–55.5 × 5–7 µm. | Ellipsoid; 7–9 × 3.5–5 µm. | Yang et al. 2023 |
| *H. pinicola* | Membranaceous, hymenial surface chalky. | Monomitic, generative hyphae with clamp connections, colorless, thin-walled | (1) Scattered; 65–180 × 7–11 µm. (2) Aseptate; 35–45 × 6–7 µm. | Cylindrical to allantoid; 13–16 × 4–4.5 µm. | Yurchenko and Wu 2014a |
| *H. puerense* | Byssoid, hymenial surface smooth, floccose. | Monomitic; generative hyphae with clamp connections, colorless, thick-walled. | Tubular; 25–97 × 5.5–9.5 µm. | Ellipsoid; 6–7.5 × 3–4.5 µm. | Guan et al. 2021 |
| *H. qujingense* | Membranaceous, hymenial surface smooth, floccose. | Monomitic; generative hyphae with clamp connections, colorless, thin-walled. | Capitate; 20–40 × 9–13 µm. | Ellipsoid to cylindrical; 7–11.5 × 3.5–5 µm. | Yang et al. 2025b |
| *H. sinense* | Membranaceous, hymenial surface smooth. | Monomitic; generative hyphae with clamp connections, colorless, thick-walled. | 1) Encrusted; 18.5–38 × 6–11 µm. 2) Moniliform; 30–60.5 × 3–5 µm. | Cylindrical to slightly allantoid; 8–11.5 × 2.6–3.3 µm | Guan and Zhao 2021b |
| *H. sordidum* | Membranaceous, hymenial surface smooth. | Monomitic; generative hyphae with clamp connections, colorless, thin-walled. | Tubular; 42–72.5 × 6–11 µm. | Ellipsoid; 3–4.5 × 2–3 µm. | Yang et al. 2023 |
| *H. tenuissimum* | Membranaceous, hymenial surface tuberculate to minutely-grandinioid | Monomitic; generative hyphae with clamp connections, colorless, thick-walled. | Cylindrical; 50–220 × 6.5–13 µm. | Cylindrical; 7–10.5 × 3–4.5 µm. | Guan et al. 2021 |
| *H. tropicum* | Coriaceous hymenial surface tuberculate. | Monomitic; generative hyphae with clamp connections, colorless, thin-walled. | Moniliform; 60–102.5 × 5.5–7.5 µm. | Ellipsoid to cylindrical; 6.5–7.5 × 3–4 µm. | Duan et al. 2023 |
| *H. weishanense* | Membranaceous, hymenial surface smooth. | Monomitic; generative hyphae with clamp connections, colorless, thin-walled. | Absent | Broadly ellipsoid; 4.5–8.5 × 4–7 µm. | Yang et al. 2023 |
| *H. yunnanense* | Corneus, hymenial surface tuberculate. | Monomitic; generative hyphae with clamp connections, colorless, thin-walled. | Cylindrical; 63–124 × 7–10 µm | Ellipsoid to cylindrical; 10–11.5 × 4–5.5 µm. | Duan et al. 2023 |

## Results

### Phylogeny of *Hyphoderma*

The ITS+nLSU dataset comprised sequences from 79 fungal specimens representing 48 species. The aligned dataset contained 2,040 characters, of which 1,414 were constant, 107 were variable but parsimony-uninformative, and 519 (25%) were parsimony-informative. Maximum parsimony analysis yielded 4,898 equally parsimonious trees (TL = 3.063, CI = 0.3389, HI = 0.6611, RI = 0.7269, and RC = 0.2463). Bayesian inference and ML analyses produced topologies largely congruent with the MP results, with an average standard deviation of split frequencies of 0.019743 for the BI analysis.

The phylogenetic tree inferred from ITS+nLSU sequences (Fig. 1) revealed that the five new taxa were grouped within the genus *Hyphoderma*. *Hyphoderma alboarachnum* was closely related to *H. floccosum* C.L. Zhao and Q.X. Guan. *Hyphoderma bambusinum* was closely related to *H. transiens* (Bres.) Parmasto. The species *H. fulgens* was closely related to *H. amoenum* (Burt) Donk. *Hyphoderma grandineum* was closely related to both *H. transiens* and *H. bambusinum*. *Hyphoderma laceratum* was closely related to *H. marginatum* Z.Y. Duan and C.L. Zhao.

This study conducted a comparative analysis of the macro- and micromorphological characteristics of the five new species and compared the morphological features with those of other *Hyphoderma* species from Yunnan Province, China (Fig. 7; Table 2).

Application of the pairwise homoplasy index (PHI) test to the combined partial ITS sequence dataset revealed no evidence of recombination among phylogenetically related species. No significant recombination events were observed between *H. alboarachnum* and *H. bambusinum* and *H. floccosum*, *H. setigerum*, *H. grandineum*, *H. transiens*, and other phylogenetically closely related species (Figs 2, 3). The test results for the combined partial ITS dataset showed that Φw = 1.0 (Φw > 0.05).

### Divergence time estimation for *Hyphoderma*

The results of divergence time estimation show (Figs 4, 5) that Polyporales emerged earlier, with a mean stem age of 163.71 Mya [95% highest posterior density (HPD) of 131.76–202.70 Mya], which is consistent with previous studies (Song and Cui 2017; Cui et al. 2025). Within Polyporales, *Hyphoderma* is closely related to the genera *Meripilus* and *Physisporinus*, with a mean stem age of 117.76 Mya (95% HPD of 92.38–147.74 Mya) and full support (1.0 PP; Figs 4, 5; Table 3).

### The historical biogeography of *Hyphoderma*

The historical biogeography scenarios inferred using RASP are shown in Fig. 6. Results of the RASP analysis suggested that Asia is likely the center of origin for *Hyphoderma* species. Among these species, 39 are found in Asia, 18 in Europe, 14 in North America, four in South America, four in Africa, and six in Oceania, suggesting that Asia remains the center of *Hyphoderma* species. In addition, the ancestral state reconstruction dataset also suggested that Asia is the ancestral region for this genus (Fig. 6).

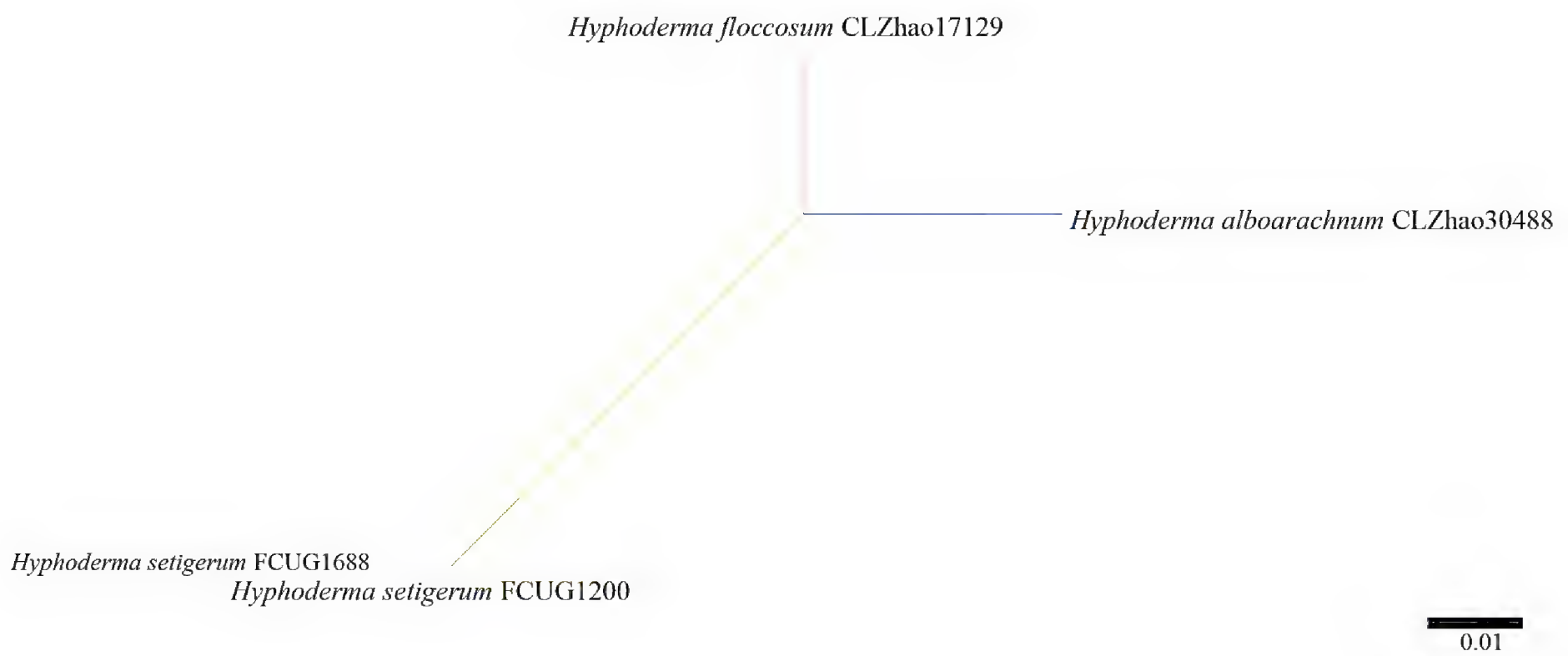


**Figure 2.** Results of the pairwise homoplasy index (PHI) test for the combined partial ITS sequence data of *Hyphoderma alboarachnum* and closely related taxa, using the LogDet transformation and splits decomposition. PHI test results (Φw ≤ 0.05) indicate significant recombination within the dataset.

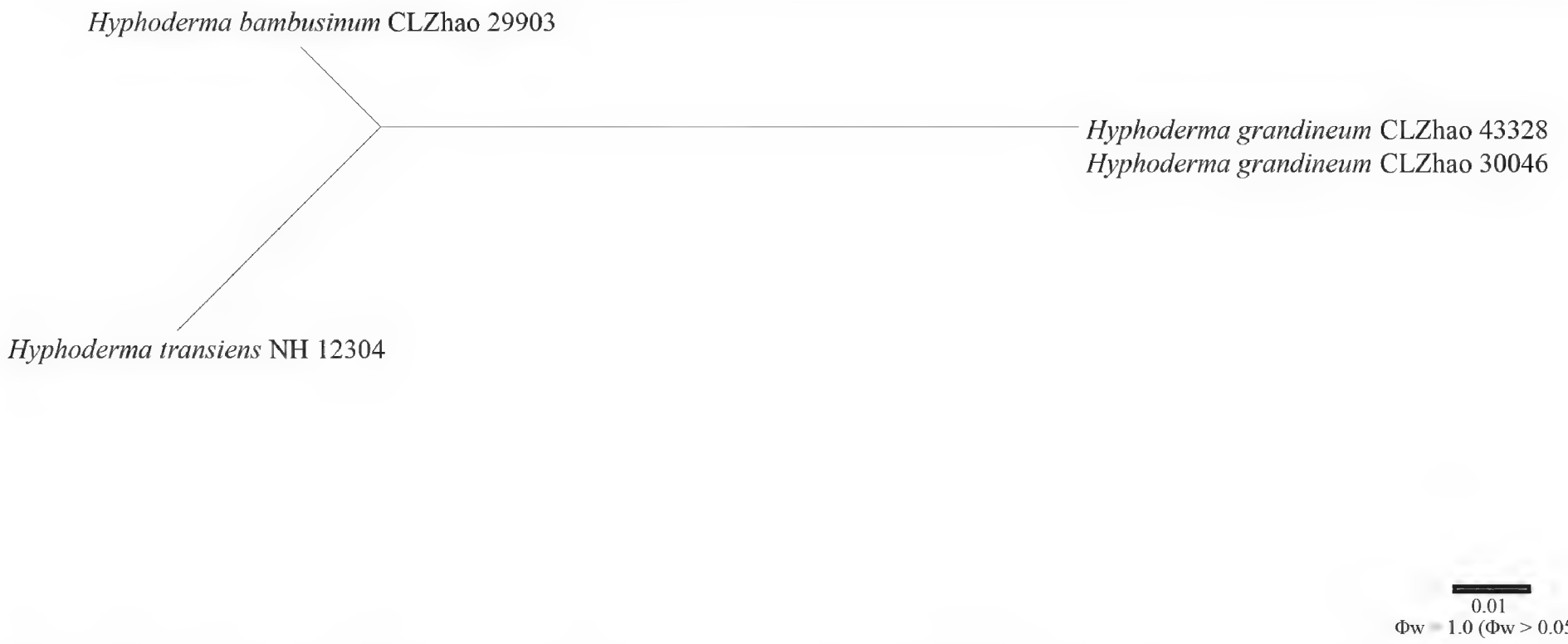


**Figure 3.** Results of the pairwise homoplasy index (PHI) test for the combined partial ITS sequence data of *Hyphoderma bambusinum* and closely related taxa, using the LogDet transformation and splits decomposition. PHI test results (Φw ≤ 0.05) indicate significant recombination within the dataset.

## Taxonomy

***Hyphoderma alboarachnum* W. Li and C.L. Zhao, sp. nov.**

MycoBank No: 859913

Figs 8, 9

**Typification.** China • Yunnan Province: Dehong, Yingjiang County, Tongbiguan Provincial Nature Reserve, GPS coordinates 24°30'N, 97°30'E, altitude 1006 m asl., on fallen angiosperm branch, leg. C.L. Zhao, 19 July 2023, CLZhao 30488 (SWFC 00030488), GenBank: ITS = PV470563.

**Etymology.** *alboarachnum* (Lat.): refers to the white basidiomata with an arachnoid hymenial surface of the type specimen.

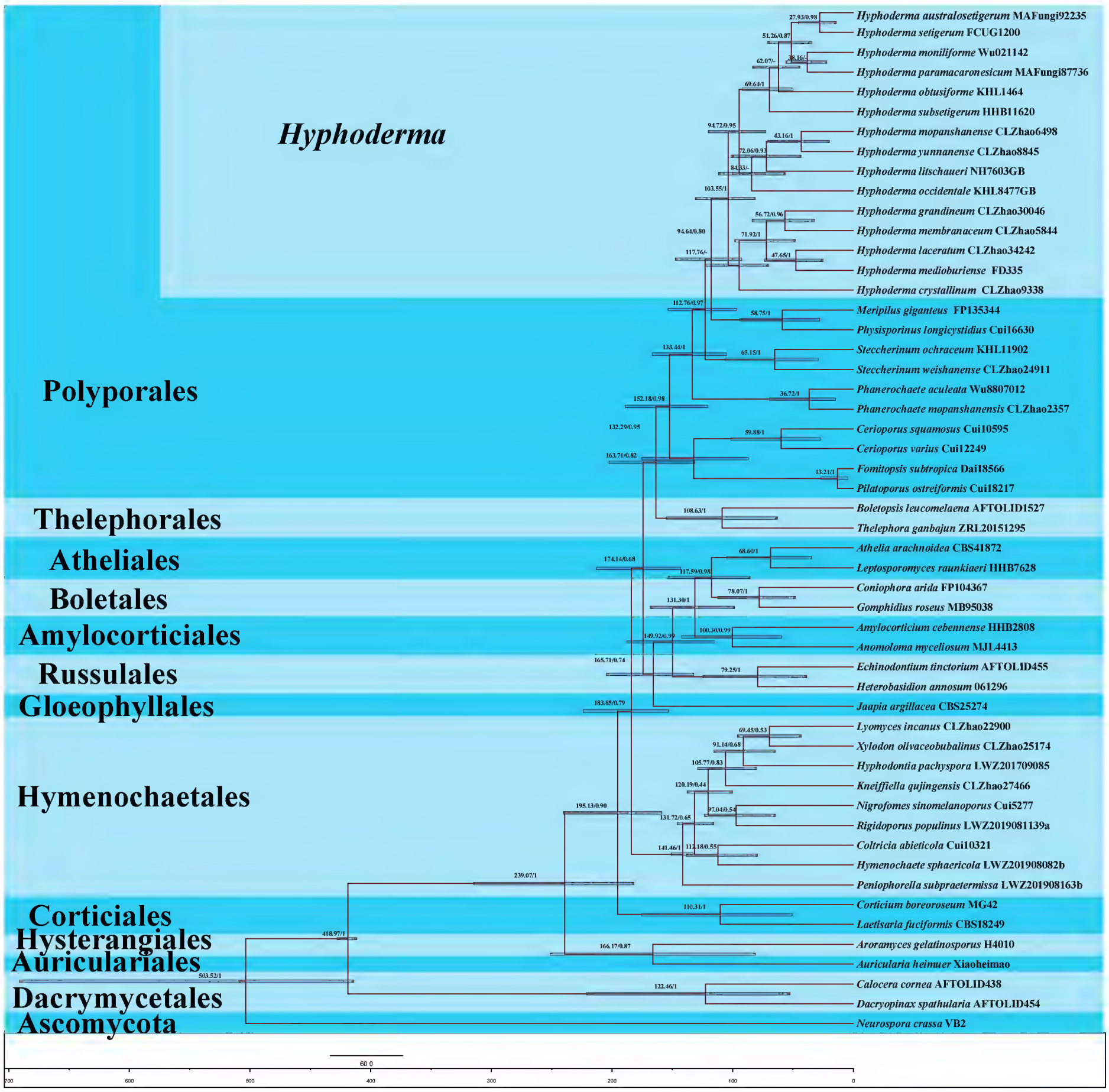


**Figure 4.** Maximum-clade-credibility chronogram and estimated divergence times of families within *Hyphoderma* inferred from the combined dataset of ITS and nLSU regions. The estimated divergence times of 95% highest posterior density are indicated as node bars for all clades and are also provided in the upper left of the tree as exact numbers for families within Hymenochaetales. Bayesian posterior probabilities above 0.7 and mean divergence times of clades (crown ages) are labeled before and after the slashes, respectively, at the nodes.

**Description.** ***Basidiomata*.** Annual, resupinate, adnate, membranaceous, without odor or taste when fresh, up to 12 cm long, 1.5 cm wide, and 100 μm thick. Hymenial surface arachnoid, white when fresh, becoming white to cream when dry. Sterile margin narrow, white, up to 1 mm.

***Hyphal system*.** Monomitic; generative hyphae with clamp connections, colorless, thin-walled, branched, interwoven, 2.5–3.5 μm in diameter, IKI–, CB–, tissues unchanged in KOH.

***Hymenium*.** Cystidia and cystidioles absent. Basidia cylindrical, colorless, thin-walled, smooth, 23.5–30 × 3.5–4.5 μm; basidioles numerous, similar to basidia in shape, but smaller.

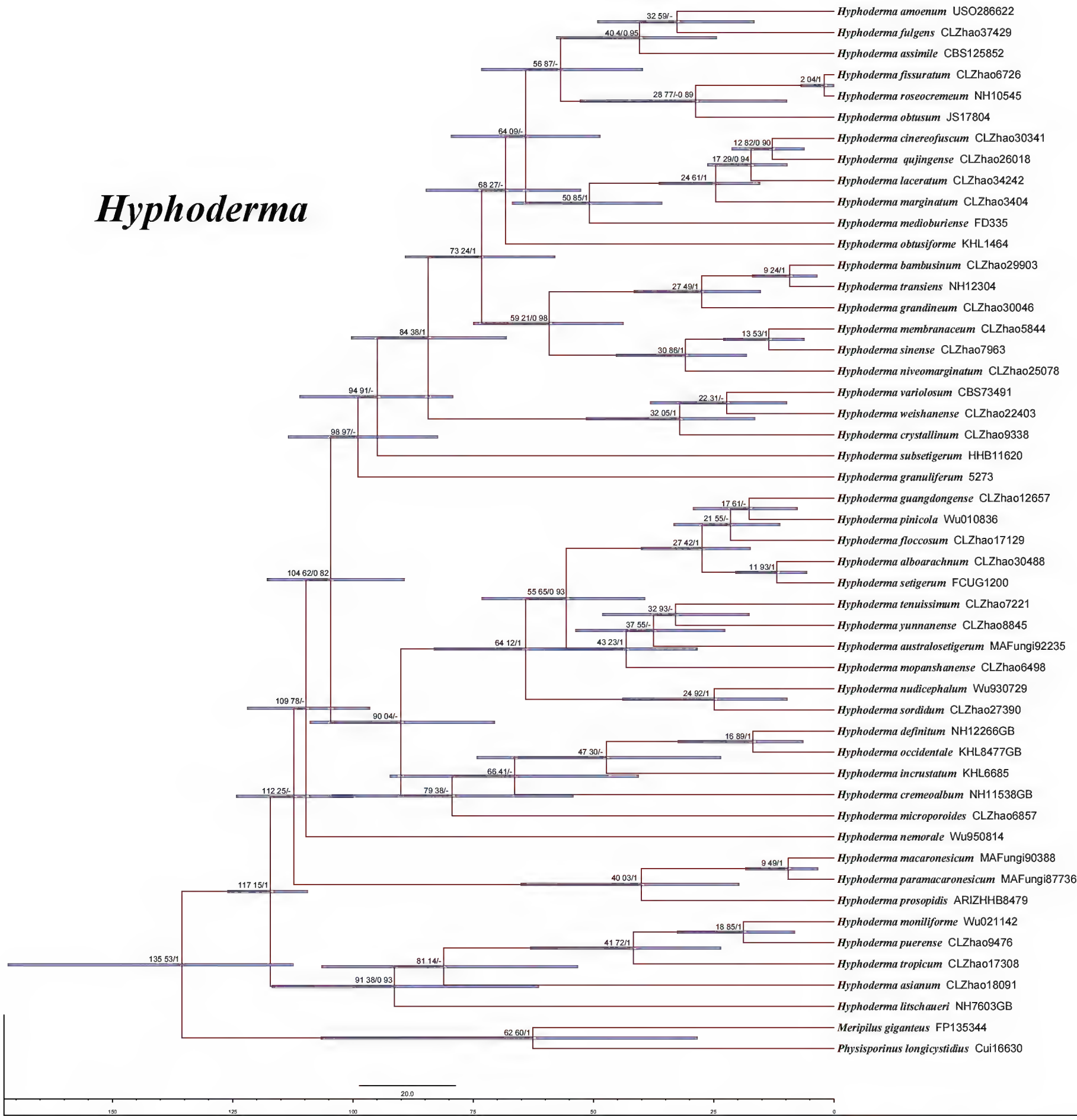


**Figure 5.** Estimated divergence times for the genus *Hyphoderma*, derived from molecular clock analyses using a combined dataset of internal transcribed spacers (ITS) and nuclear large ribosomal subunit (nLSU) sequences. Mean divergence times (Ma) and posterior probabilities (PP) > 0.8 are annotated at the internodes, with horizontal blue bars representing the 95% highest posterior density (HPD) intervals for divergence time estimates.

***Spores*.** Basidiospores oblong-ellipsoid to cylindrical, colorless, thin-walled, smooth, with inner oil droplets, IKI–, CB–, 5–6(–6.5) × 2–3 µm, L = 5.59 µm, W = 2.66 µm, Q = 2.25 (n = 30/1).

**Notes.** In the phylogenetic analysis (Fig. 1), *Hyphoderma alboarachnum* (CLZhao 30488) was closely related to and formed a sister lineage with *H. floccosum* (CLZhao 17129, CLZhao 17215), with 100% ML, 91 MP bootstrap support, and a 1.00 BYPP value. However, morphologically, *H. floccosum* differs from *H. alboarachnum* by having a farinaceous hymenial surface and larger basidiospores (5–6 × 2–3 µm vs. 6–9.5 × 3–4.5 µm; Guan and Zhao 2021b). In addition, the latter was found in the Wenshan National Nature

**Table 3.** The estimated divergence times of the genus of *Hyphoderma*.

| Taxa | Means of stem age (Ma) | 95% HPD (Ma) |
|---|---|---|
| *Hyphoderma alboarachnum* | 11.93 | 5.57–20.46 |
| *H. amoenum* | 32.59 | 16.57–49.20 |
| *H. asianum* | 81.14 | 53.20–106.54 |
| *H. assimile* | 40.40 | 24.36–57.71 |
| *H. australosetigerum* | 37.55 | 22.63–53.73 |
| *H. bambusinum* | 9.24 | 3.42–17.02 |
| *H. cinereofuscum* | 12.82 | 6.16–21.28 |
| *H. cremeoalbum* | 66.41 | 40.63–92.33 |
| *H. crystallinum* | 32.05 | 16.41–51.53 |
| *H. definitum* | 16.89 | 6.40–32.47 |
| *H. fissuratum* | 2.04 | 0.02–6.92 |
| *H. floccosum* | 21.55 | 11.21–33.35 |
| *H. fulgens* | 32.59 | 16.57–49.20 |
| *H. granuliferum* | 98.97 | 82.33–113.44 |
| *H. grandineum* | 27.49 | 15.22–41.59 |
| *H. guangdongense* | 17.61 | 7.59–29.35 |
| *H. incrustatum* | 47.30 | 23.50–74.28 |
| *H. laceratum* | 17.29 | 9.71–26.31 |
| *H. litschaueri* | 91.38 | 61.37–116.85 |
| *H. macaronesicum* | 9.49 | 3.33–18.47 |
| *H. marginatum* | 24.61 | 15.35–36.42 |
| *H. medioburiense* | 50.85 | 35.70–66.97 |
| *H. membranaceum* | 13.53 | 6.11–22.98 |
| *H. microporoides* | 79.38 | 54.13–104.43 |
| *H. moniliforme* | 18.85 | 8.07–32.66 |
| *H. mopanshanense* | 43.23 | 28.40–60.09 |
| *H. nemorale* | 112.25 | 96.42–121.98 |
| *H. niveomarginatum* | 30.86 | 18.16–45.31 |
| *H. nudicephalum* | 24.92 | 9.68–43.99 |
| *H. obtusiforme* | 66.27 | 52.57–84.85 |
| *H. obtusum* | 28.77 | 9.77–52.86 |
| *H. occidentale* | 16.89 | 6.40–32.47 |
| *H. paramacaronesicum* | 9.49 | 3.33–18.47 |
| *H. pinicola* | 17.61 | 7.59–29.35 |
| *H. prosopidis* | 40.03 | 19.71–65.11 |
| *H. puerense* | 18.85 | 8.07–32.66 |
| *H. qujingense* | 12.82 | 6.16–21.28 |
| *H. roseocremeum* | 2.04 | 0.02–6.92 |
| *H. setigerum* | 11.93 | 5.57–20.46 |
| *H. sinense* | 13.53 | 6.11–22.98 |
| *H. sordidum* | 24.92 | 9.68–43.99 |
| *H. subsetigerum* | 94.91 | 79.13–111.14 |
| *H. tenuissimum* | 32.93 | 17.60–48.15 |
| *H. transiens* | 9.24 | 3.42–17.02 |
| *H. tropicum* | 41.72 | 23.45–63.12 |
| *H. variolosum* | 22.31 | 9.77–38.21 |
| *H. weishanense* | 22.31 | 9.77–38.21 |
| *H. yunnanense* | 32.93 | 17.60–48.15 |

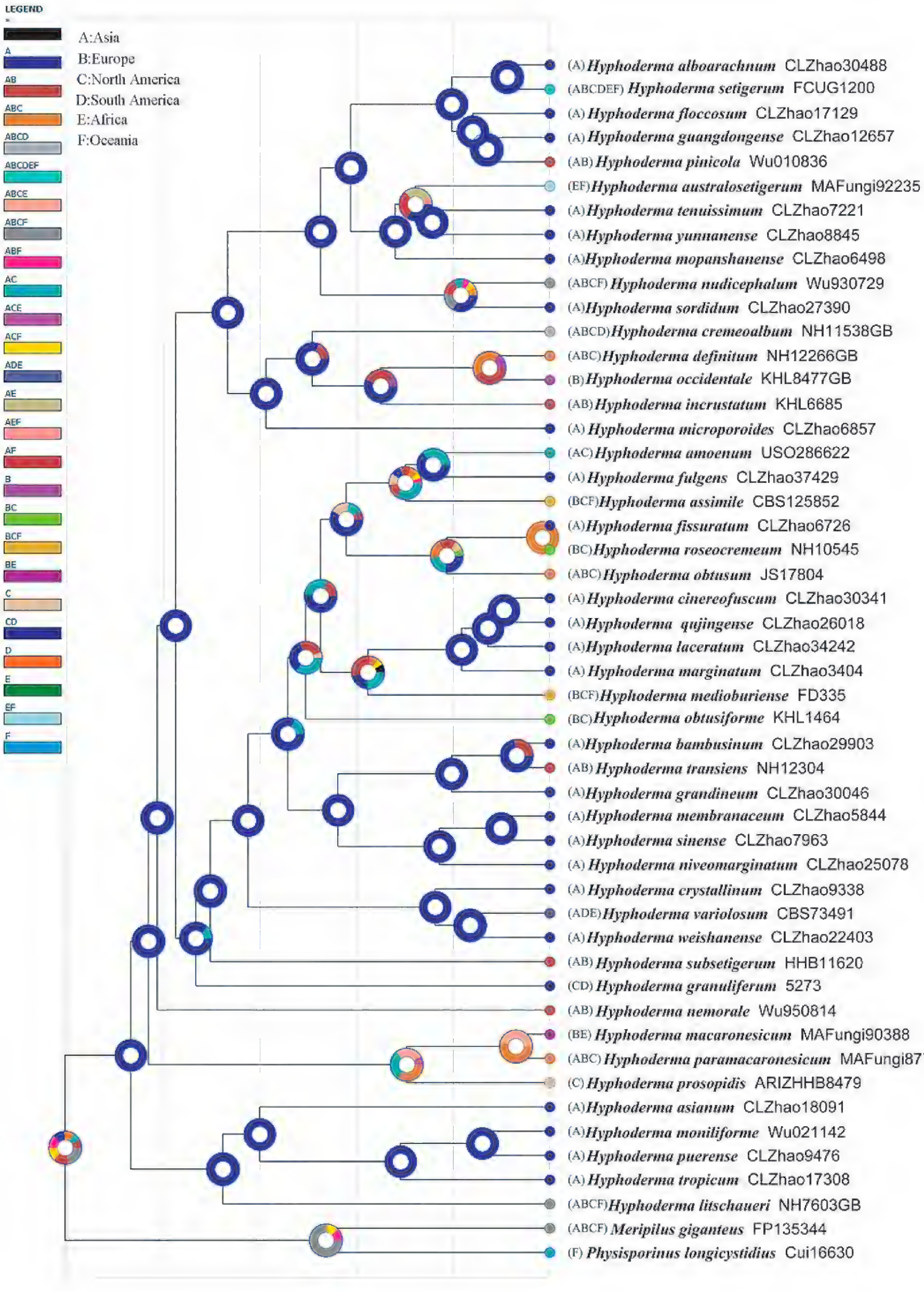


**Figure 6.** Ancestral state reconstruction of *Hyphoderma* conducted to determine (**A**) the origin center and (**B**) the origin host trees using a dataset comprising internal transcribed spacers (ITS) and nuclear large ribosomal subunit (nLSU) sequences. At each node, a pie chart represents the possible ancestral distributions inferred from dispersal–extinction–cladogenesis (DEC) analyses, as implemented in Reconstruct Ancestral State in Phylogenies (RASP).

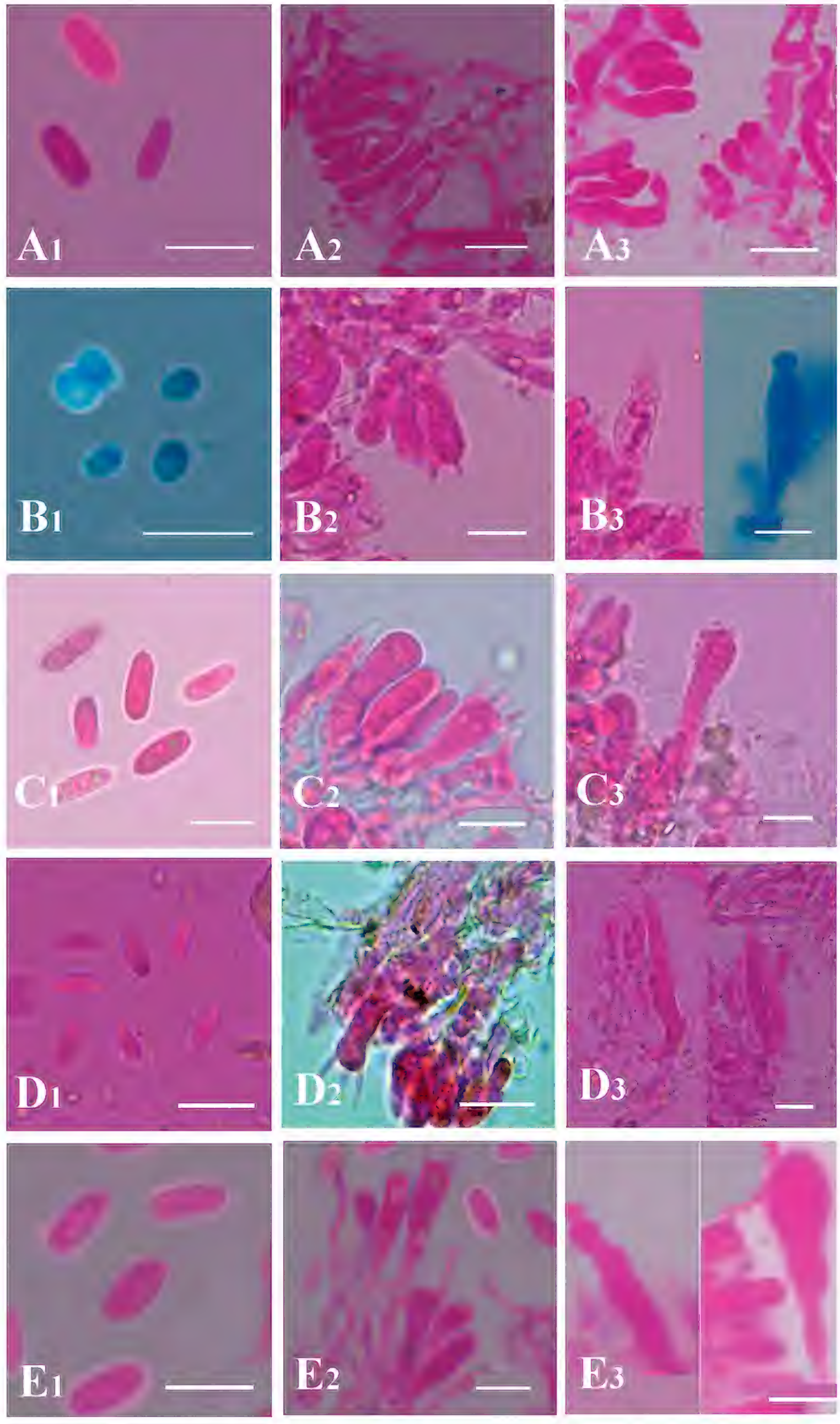


**Figure 7.** Comparison of micromorphological characteristics among the five new *Hyphoderma* species. **A1–A3.** *Hyphoderma alboarachnum*; **B1–B3.** *Hyphoderma bambusinum*; **C1–C3.** *Hyphoderma fulgens*; **D1–D3.** *Hyphoderma grandineum*; **E1–E3.** *Hyphoderma laceratum*. Scale bars: 10 μm (**A1–E3**).

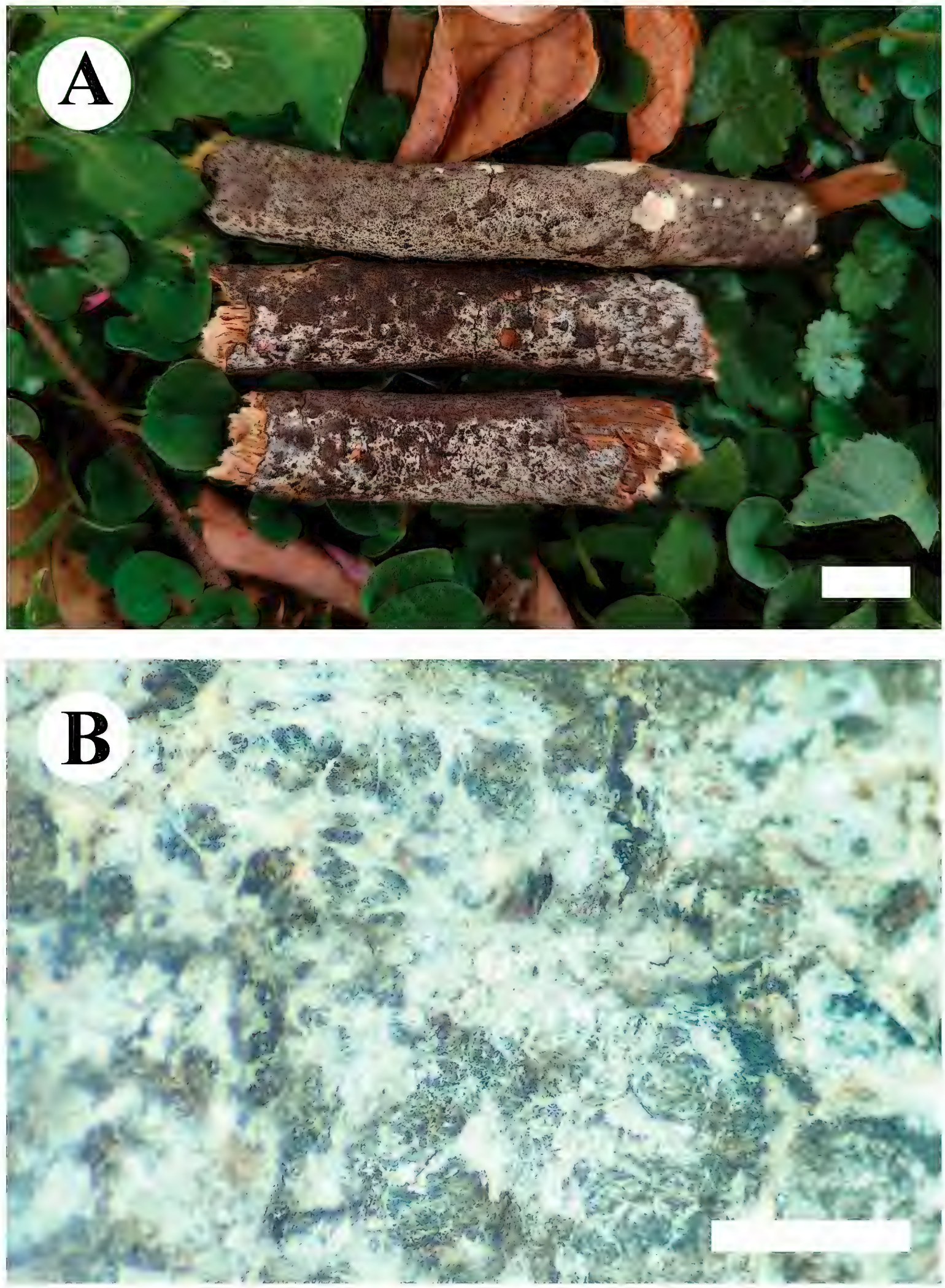


**Figure 8.** Basidiomata of *Hyphoderma alboarachnum* (holotype CLZhao 30488). Scale bars: 1 cm (**A**); 1 mm (**B**).

Reserve at an altitude of 2,480 m. Morphologically, *H. alboarachnum* is similar to *H. mopanshanense* and *H. membranaceum* in having subellipsoid to cylindrical basidiospores (Guan and Zhao 2021a; Ma et al. 2021). However, *H. mopanshanense* is distinguished from *H. alboarachnum* by its ceraceous hymenial surface and longer basidiospores (7.8–9.7 × 2.6–3.3 µm vs. 5–6 × 2–3 µm; Ma et al. 2021). The species *H. membranaceum* differs from *H. alboarachnum* by its tuberculate hymenial surface and larger basidiospores (11–13.5 × 4.5–5.5 µm vs. 5–6 × 2–3 µm; Guan and Zhao 2021a). Thus, based on morphological and phylogenetic evidence, we introduce our collection as a new species, *Hyphoderma alboarachnum*.

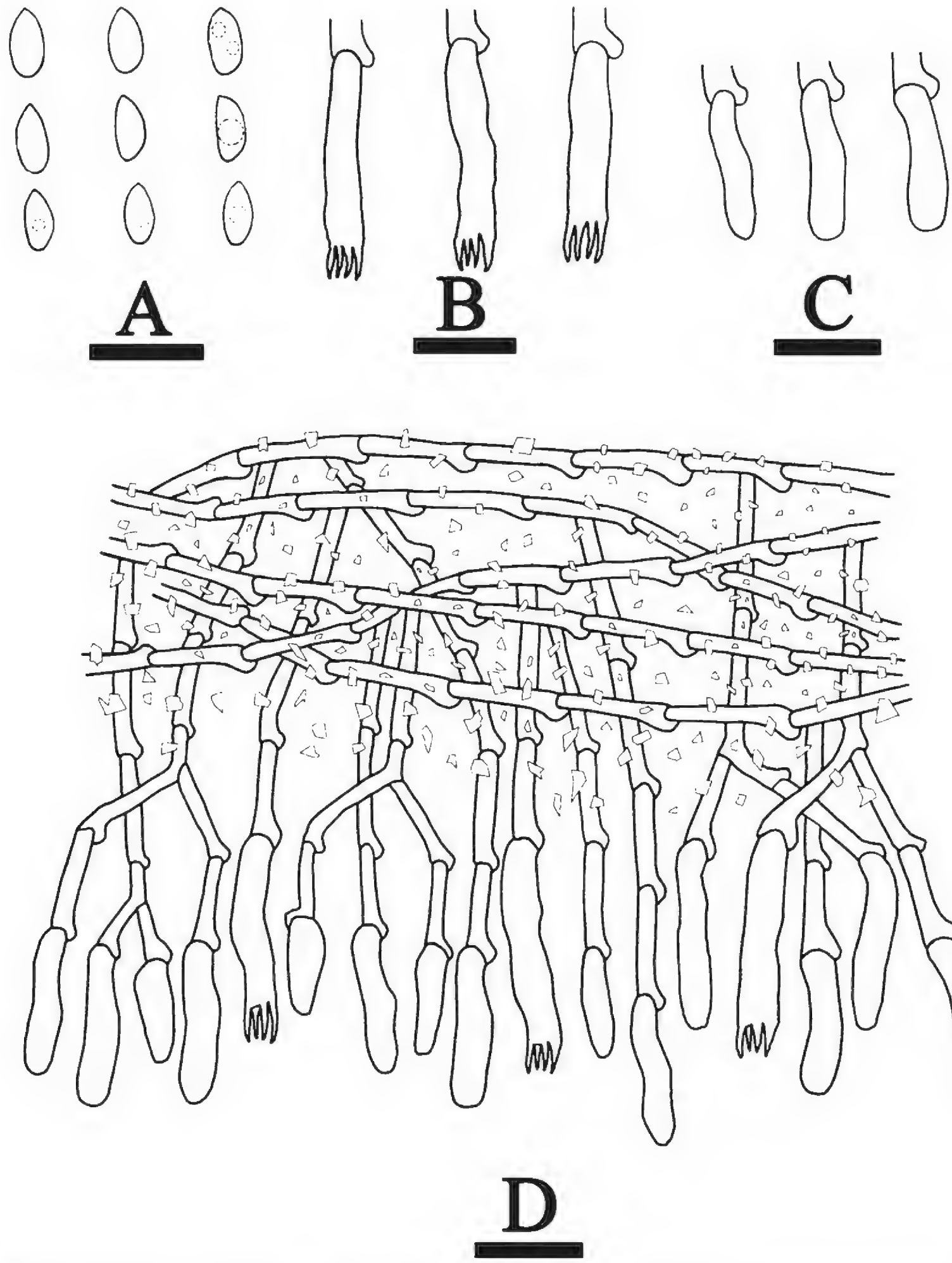


**Figure 9.** Microscopic structures of *Hyphoderma alboarachnum* (holotype CLZhao 30488). **A.** Basidiospores; **B.** Basidia; **C.** Basidioles; **D.** Part of a vertical section of the hymenium. Scale bars: 10 μm (**A–D**).

***Hyphoderma bambusinum* W. Li and C.L. Zhao, sp. nov.**

MycoBank No: 859914

Figs 10, 11

**Typification.** China • Yunnan Province: Dehong, Yingjiang County, Tongbiguan Provincial Nature Reserve, GPS coordinates 24°30'N, 97°30'E, altitude 1006 m asl., on dead bamboo, leg. C.L. Zhao, 18 July 2023, CLZhao 29903 (SWFC 00029903), GenBank: ITS = PV469674; nLSU = PV819428.

**Etymology.** *bambusinum* (Lat.) refers to the host bamboo on which the fungal species grows.

**Description.** ***Basidiomata*.** Annual, resupinate, adnate, membranaceous, without odor or taste when fresh, up to 7 cm long, 2.5 cm wide, and 100 μm thick. Hymenial surface smooth, white to cream when fresh, becoming cream to buff when dry. Sterile margin narrow, white to cream, up to 1 mm.

***Hyphal system*.** Monomitic; generative hyphae with clamp connections, colorless, thick, branched, interwoven, 2.5–3 μm in diameter, IKI–, CB–, tissues unchanged in KOH.

***Hymenium*.** Cystidia tubular, colorless, thin-walled, smooth, 21.5–26.5 × 5–6.5 μm. Basidia subclavate to subcylindrical, thin-walled, smooth, slightly flexuous, with four sterigmata and a simple septum at the base, 16–17.5 × 3.5–5.5 μm; basidioles similar to basidia in shape but slightly smaller.

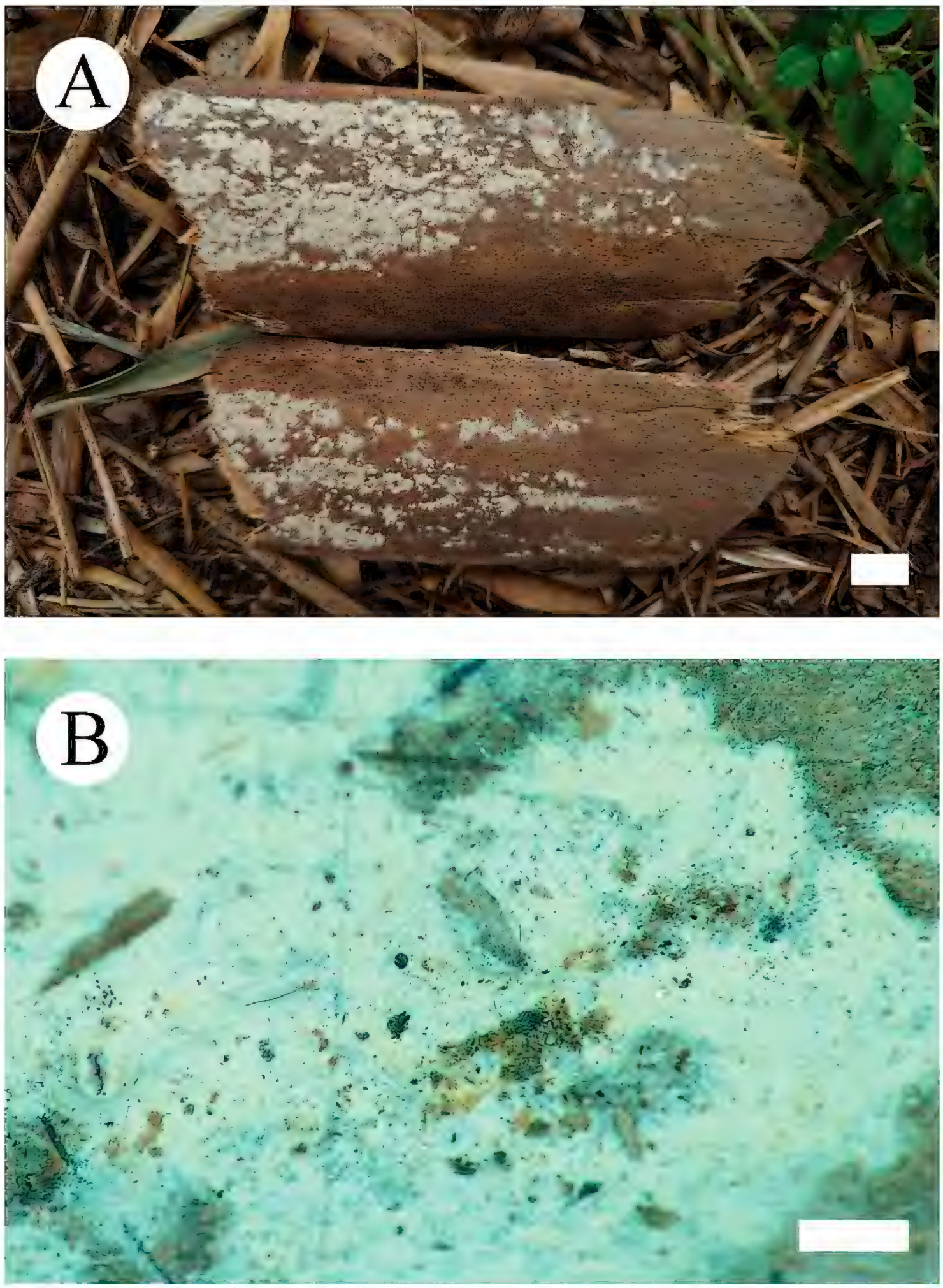


**Figure 10.** Basidiomata of *Hyphoderma bambusinum* (holotype CLZhao 29903). Scale bars: 1 cm (**A**); 1 mm (**B**).

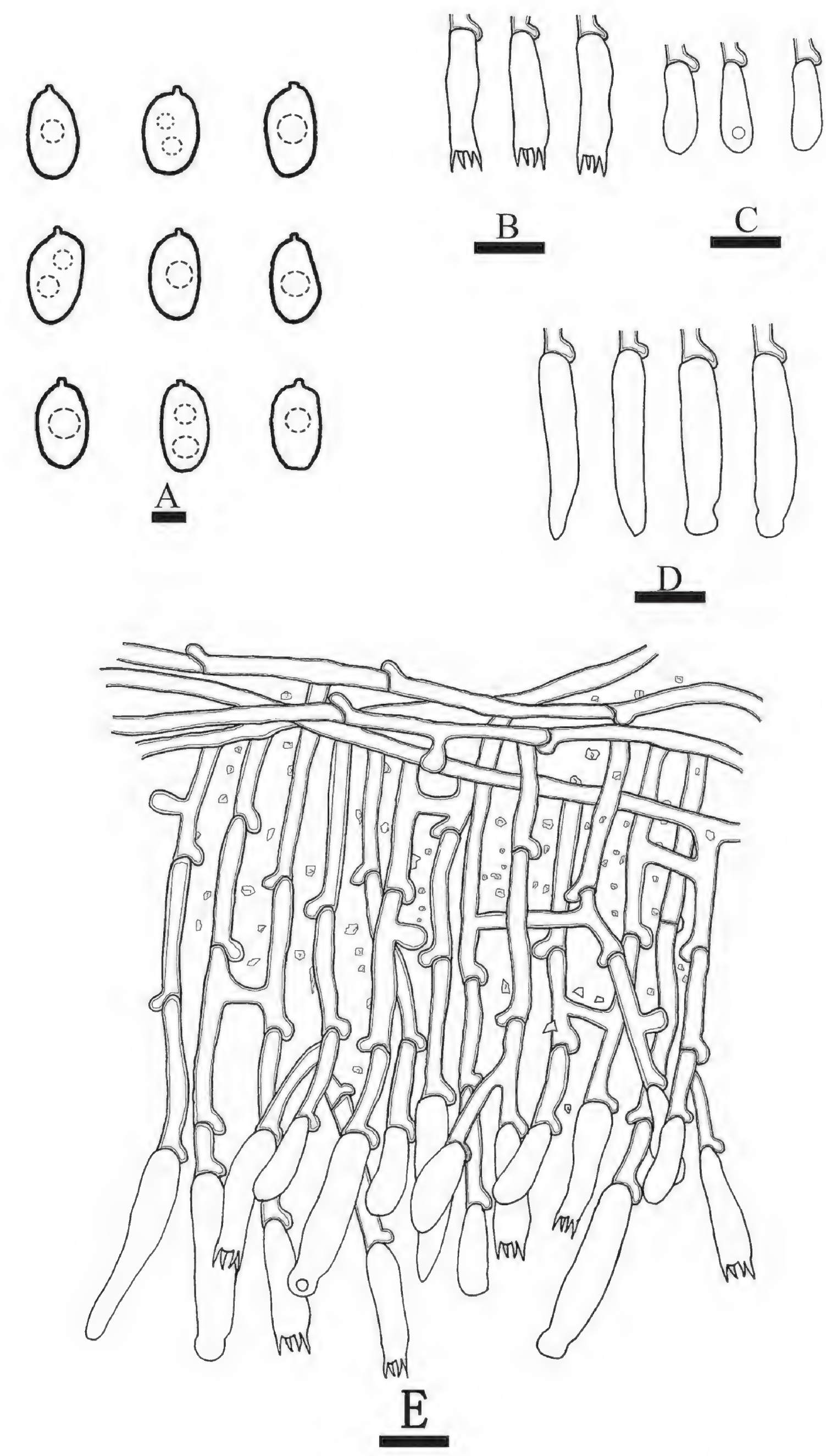


**Figure 11.** Microscopic structures of *Hyphoderma bambusinum* (holotype CLZhao 29903). **A.** Basidiospores; **B.** Basidia; **C.** Basidioles; **D.** Cystidia; **E.** Part of a vertical section of the hymenium. Scale bars: 2 μm (**A**); 10 μm (**B–E**).

***Spores*.** Basidiospores ellipsoid, colorless, thin-walled, smooth, with oil droplets inside, IKI–, CB–, 4.5–6.5 × 3–4.5(–5) µm, L = 5.55 µm, W = 3.78 µm, Q = 1.47 (n = 30/1).

**Notes.** *Hyphoderma bambusinum* (CLZhao 29903) was found to be phylogenetically closely related to *H. transiens* (NH 12304 [GB]), with 100% ML, 100 MP bootstrap support, and a 1.00 BYPP value. However, morphologically, *H. transiens* differs from *H. bambusinum* by having an odontioid hymenial surface and longer basidiospores (9–13 × 3–4.5 µm vs. 4.5–6.5 × 3–4.5 µm; Parmasto 1968); additionally, the latter was found in Portugal and growing on the bark of *Quercus*. Morphologically, *H. bambusinum* is similar to *H. cremeoalbum* (Höhn. and Litsch.) Jülich. and *H. floccosum* by having ellipsoid basidiospores (Bernicchia and Gorjón 2010; Guan and Zhao 2021b). However, *H. cremeoalbum* is distinguished from *H. bambusinum* by its larger basidiospores (10–14 × 5–6.5 µm vs. 4.5–6.5 × 3–4.5 µm; Bernicchia and Gorjón 2010). The species *H. floccosum* differs from *H. bambusinum* by its ceraceous basidiomata and longer, tubular cystidia (37.5–100 × 4–8.5 µm vs. 21.5–26.5 × 5–6.5 µm; Guan and Zhao 2021b). These morphological differences, together with phylogenetic analyses, support the conclusion that our taxon represents a new species, *Hyphoderma bambusinum*.

### *Hyphoderma fulgens* W. Li and C.L. Zhao, sp. nov.

MycoBank No: 859915

Figs 12, 13

**Typification.** China • Yunnan Province: Dehong, Yingjiang County, Tongbiguan Provincial Nature Reserve, GPS coordinates 24°30'N, 97°30'E, altitude 1006 m asl., on fallen angiosperm branch, leg. C.L. Zhao, 3 July 2024, CLZhao 37429 (SWFC 00037429), GenBank: ITS = PV829544; nLSU = PV810095.

**Etymology.** *fulgens* (Lat.): refers to the shiny color of the hymenial surface of the specimens.

**Description.** ***Basidiomata*.** Annual, resupinate, adnate, membranaceous, without odor or taste when fresh, up to 9 cm long, 1.8 cm wide, and 100 µm thick. Hymenial surface smooth, white to cream when fresh, white when dry. Sterile margin narrow, white, up to 1 mm.

***Hyphal system*.** Monomitic; generative hyphae with clamp connections, colorless, thin-walled, branched, interwoven, 2.5–3.2 µm in diameter, IKI–, CB–, tissues unchanged in KOH.

***Hymenium*.** Cystidia clavate, colorless, thin-walled, smooth, encrusted, 30.4–37.1 × 5.5–7.5 µm. Basidia barreled, thin-walled, smooth, slightly flexuous, with four sterigmata and a simple septum at the base, 21.5–26 × 5.5–8 µm; basidioles similar to basidia in shape but slightly smaller.

***Spores*.** Basidiospores subcylindrical, colorless, thin-walled, smooth, with oil droplets inside, IKI–, CB–, (7–)7.5–11.5 × (2–)2.5–4 µm, L = 9.55 µm, W = 3.39 µm, Q = 2.74–2.89 (n = 120/4).

**Additional specimens examined (paratypes).** China • Yunnan Province: Dehong, Yingjiang County, Tongbiguan Provincial Nature Reserve, GPS coordinates 24°30'N, 97°30'E, altitude 1006 m asl., on fallen angiosperm branch, leg. C.L. Zhao, 19 July 2023, CLZhao 30254 (SWFC 00030254); 2 July 2024, CLZhao

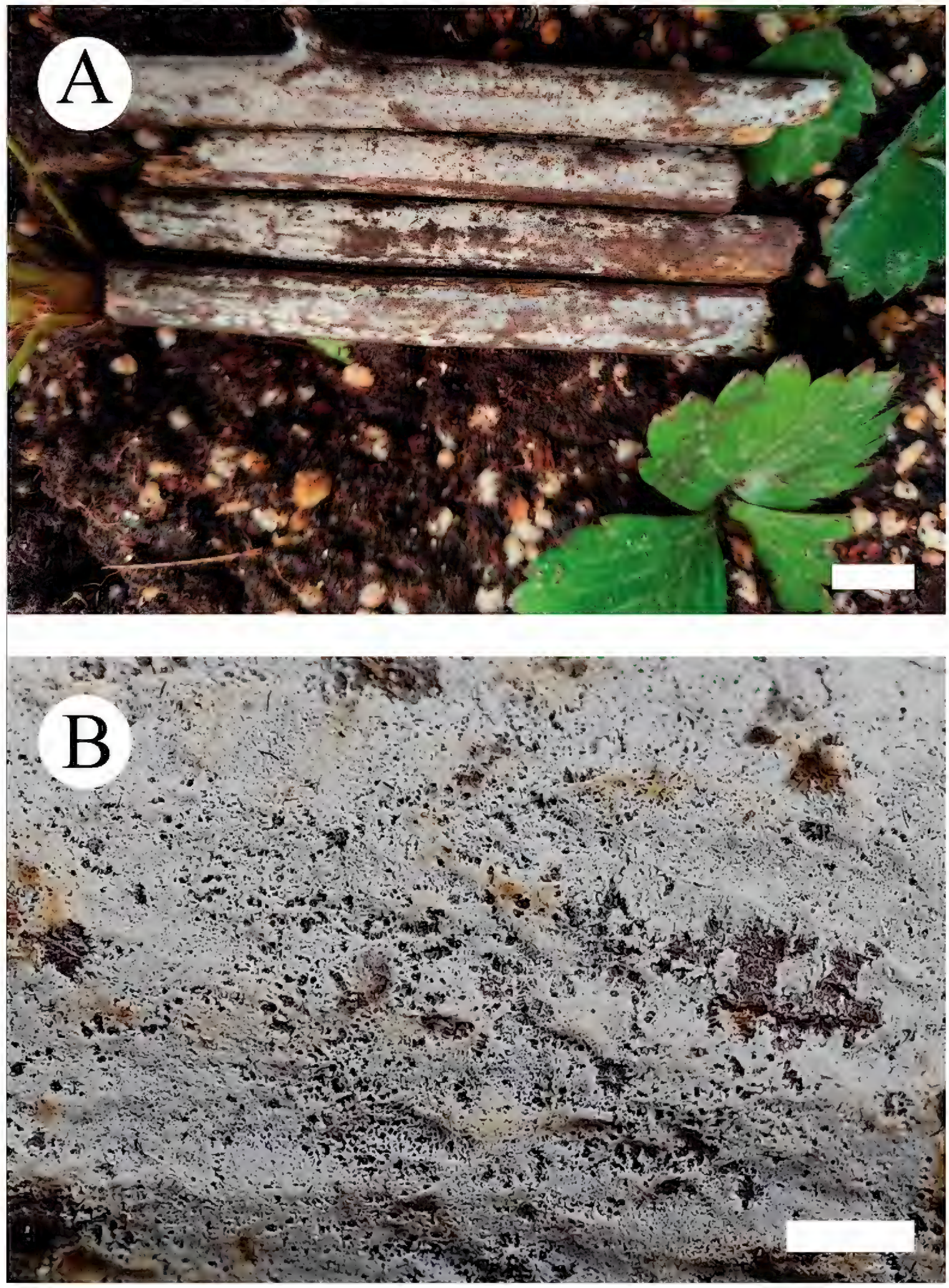


**Figure 12.** Basidiomata of *Hyphoderma fulgens* (holotype CLZhao 37429). Scale bars: 1 cm (**A**); 1 mm (**B**).

37266 (SWFC 00037266); • Mang City, Tongbiguan Provincial Nature Reserve, GPS coordinates 24°42'N, 97°54'E, altitude 1006 m asl., on fallen angiosperm branch, leg. C.L. Zhao, 29 June 2024, CLZhao 36600 (SWFC 00036600); 8 July 2024, CLZhao 39677 (SWFC 00039677); CLZhao 39618 (SWFC 00039618); CLZhao 39474 (SWFC 00039474).

**Notes.** In the phylogenetic analysis, the specimens of *Hyphoderma fulgens* (CLZhao 37429, CLZhao 30254, CLZhao 36600, CLZhao 39474) formed a closely related sister relationship to *H. amoenum* (Burt) Donk (USO 286622), with 99% ML, 89 MP bootstrap support, and a 0.99 BYPP value. However, morphologically, *H. amoenum* differs from *H. fulgens* by having

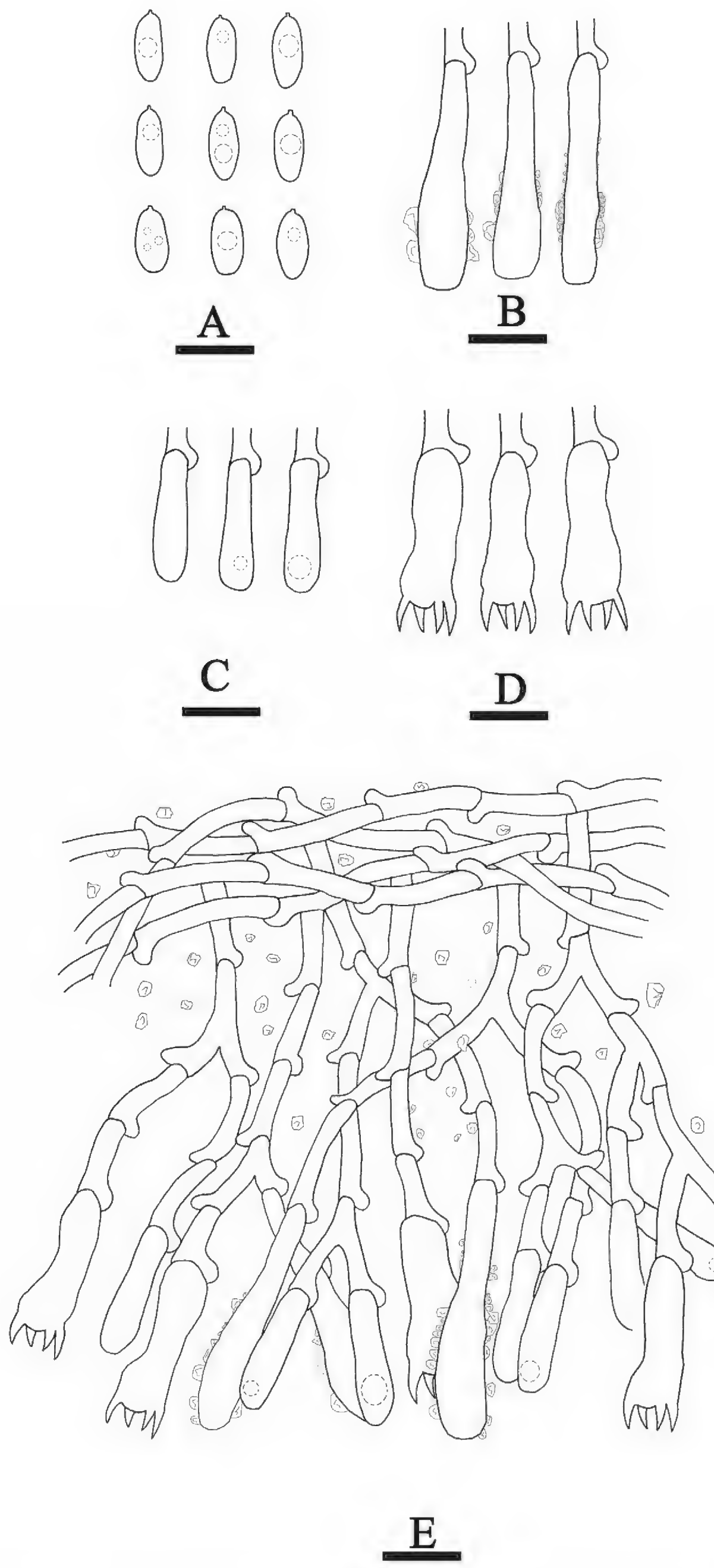


**Figure 13.** Microscopic structures of *Hyphoderma fulgens* (holotype CLZhao 37429). **A.** Basidiospores; **B.** Cystidia; **C.** Basidioles; **D.** Basidia; **E.** Part of a vertical section of the hymenium. Scale bars: 10 μm (**A–E**).

wider basidiospores (9–13 × 5–6 µm vs. 7.5–11.5 × 2.5–4 µm; Tellería et al. 2012). Morphologically, *H. fulgens* is similar to *H. guangdongense* and *H. tenuissimum* by having subcylindrical basidiospores (Guan and Zhao 2021a; Su et al. 2024). However, *H. guangdongense* is distinguished from *H. fulgens* by its farinaceous hymenial surface and septate cystidia (Su et al. 2024). In addition, *H. tenuissimum* differs from *H. fulgens* by its tuberculate to minutely grandinioid hymenial surface and larger cystidia (50–220 × 6.5–13 µm vs. 30.4–37.1 × 5.5–7.5 µm; Guan and Zhao 2021a). These morphological and phylogenetic data indicate that our collections represent a new species, *Hyphoderma fulgens*.

***Hyphoderma grandineum* W. Li and C.L. Zhao, sp. nov.**

MycoBank No: 859916

Figs 14, 15

**Typification.** China • Yunnan Province: Dehong, Yingjiang County, Tongbiguan Provincial Nature Reserve, GPS coordinates 24°30'N, 97°30'E, altitude 1006 m asl., on the fallen angiosperm branch, leg. C.L. Zhao, 18 July 2023, CLZhao 30046 (SWFC 00030046), GenBank: ITS = PV470561, nLSU = PV819429.

**Etymology.** *grandineum* (Lat.): refers to the grandinioid hymenial surface of the type specimen.

**Description.** ***Basidiomata*.** Annual, resupinate, adnate, membranaceous, without odor or taste when fresh, up to 7.5 cm long, 2 cm wide, and 100 µm thick. Hymenial surface grandinioid, cream when fresh, becoming cream to yellowish when dry. Sterile margin narrow, white, up to 1 mm.

***Hyphal system*.** Monomitic; generative hyphae with clamp connections, colorless, thin-walled, branched, interwoven, 3–3.6 µm in diameter, IKI–, CB–, tissues unchanged in KOH.

***Hymenium*.** Leptocystidia, colorless, thin-walled, smooth, 29.5–33.5 × 4–5 µm. Basidia clavate, thin-walled, smooth, slightly flexuous, with four sterigmata and a simple septum at the base, 18–19.5 × 4.5–6 µm; basidioles similar to basidia in shape but slightly smaller.

***Spores*.** Basidiospores cylindrical, colorless, thin-walled, smooth, IKI–, CB–, (6–)7–9 × 2.5–4 µm, L = 7.9 µm, W = 3.2 µm, Q = 2.48–2.5 (n = 60/2).

**Additional specimen examined (paratype).** China • Yunnan Province: Dehong, Ruili City, Tongbiguan Provincial Nature Reserve, GPS coordinates 23°22'N, 97°18'E, altitude 976 m asl., on the fallen angiosperm branch, leg. C.L. Zhao, 2 December 2024, CLZhao 43328(SWFC 00043328), GenBank: ITS = PV470562, nLSU = PV819430.

**Notes.** In the phylogenetic analysis, *Hyphoderma grandineum* (CLZhao 30046, CLZhao 43328) formed a closely related sister relationship with the clade consisting of *H. transiens* (Bres.) Parmasto (NH 12304 [GB]) and *H. bambusinum* (CLZhao 29903), with 100% ML, 100 MP bootstrap support, and a 1.00 BYPP value. However, morphologically, *H. transiens* differs from *H. grandineum* by having a whitish to ochraceous hymenial surface and longer basidiospores (9–13 × 3–4.5 µm vs. 7–9 × 2.5–4 µm; Parmasto 1968); in addition, the latter was found in Portugal. Morphologically, *H. grandine-*

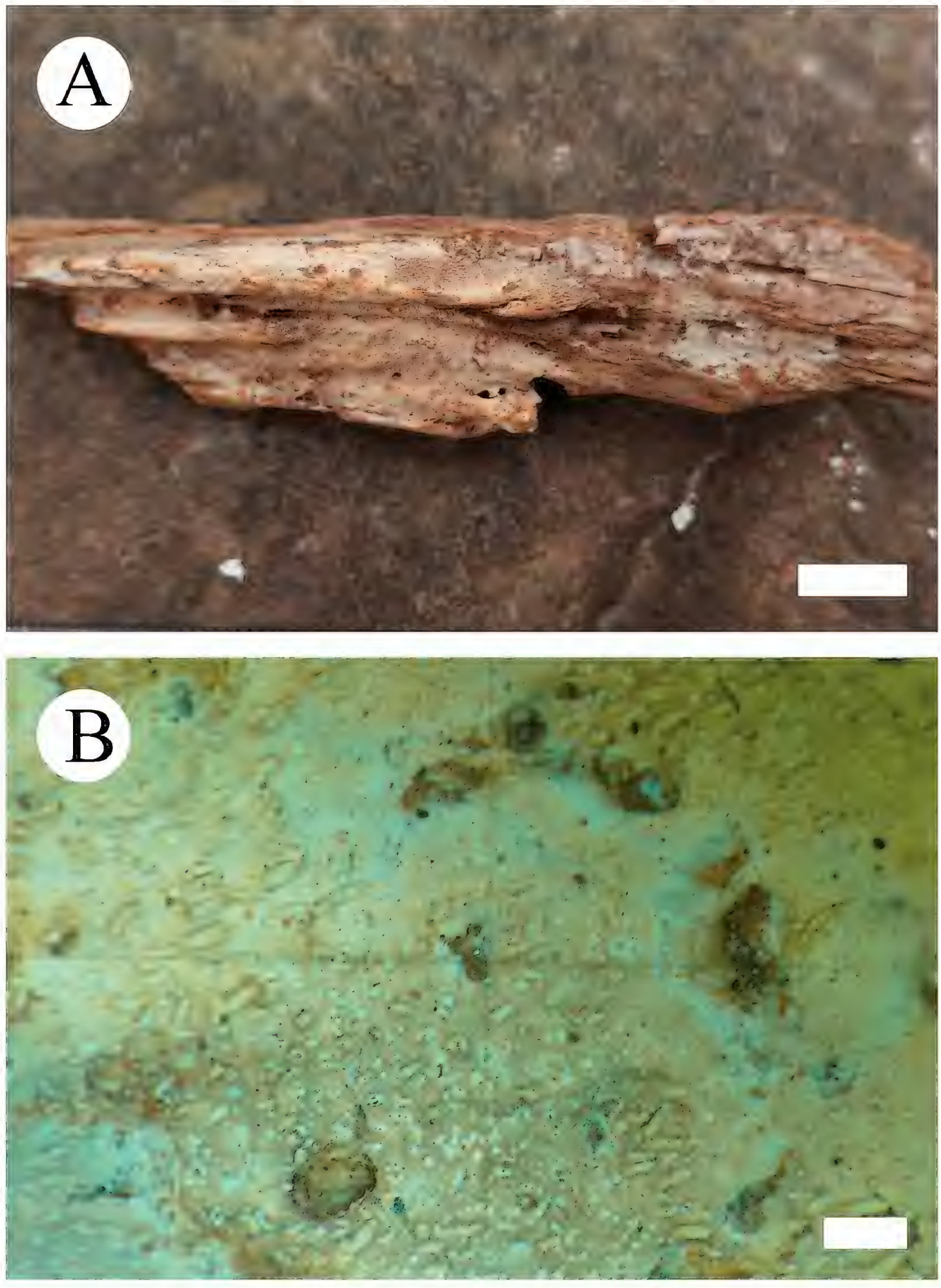


**Figure 14.** Basidiomata of *Hyphoderma grandineum* (holotype CLZhao 30046). Scale bars: 1 cm (**A**); 1 mm (**B**).

*um* is similar to *H. tropicum* and *H. tenuissimum* by having a tuberculate to odontoid hymenial surface (Guan et al. 2021; Duan et al. 2023). However, *H. tropicum* is distinguished from *H. grandineum* by its coriaceous hymenial surface and moniliform cystidia (Duan et al. 2023). In addition, *H. tenuissimum* differs from *H. grandineum* by its larger cystidia (50–220 × 6.5–13 µm vs. 29.5–33.5 × 4–5 µm; Guan et al. 2021). These morphological and phylogenetic evidences show that our collections represent a new species, *Hyphoderma grandineum*.

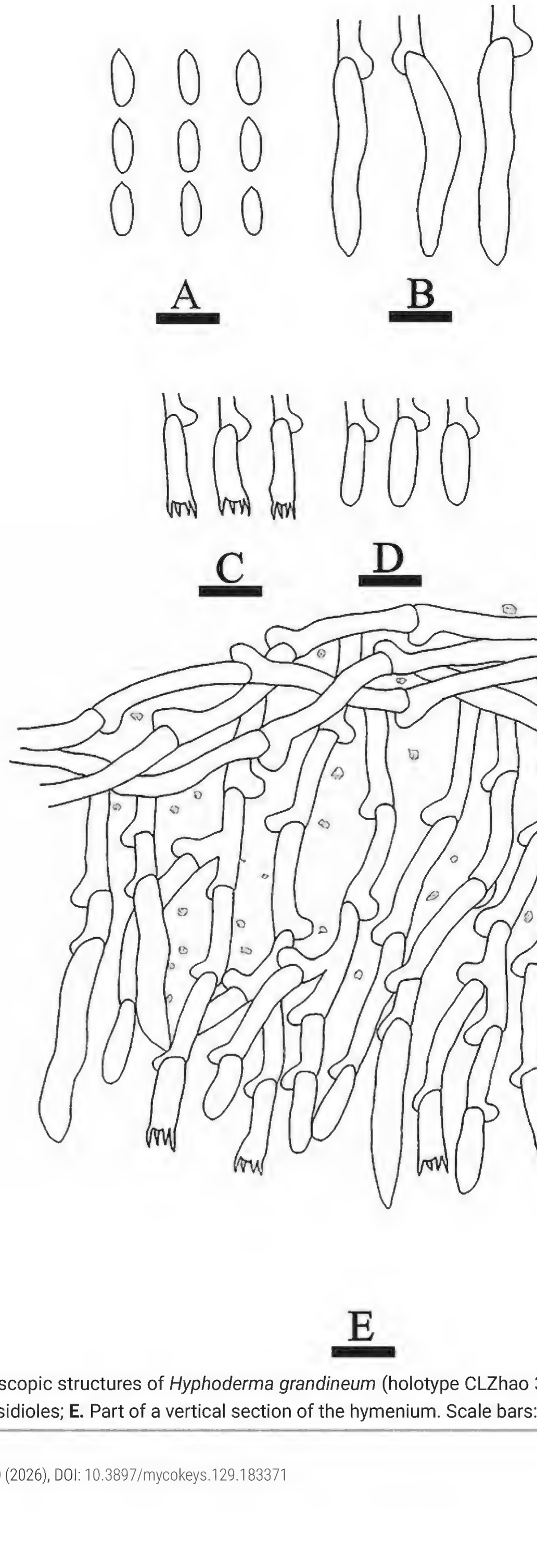


**Figure 15.** Microscopic structures of *Hyphoderma grandineum* (holotype CLZhao 30046). **A.** Basidiospores; **B.** Cystidia; **C.** Basidia; **D.** Basidioles; **E.** Part of a vertical section of the hymenium. Scale bars: 10 μm (**A–E**).

***Hyphoderma laceratum* W. Li and C.L. Zhao, sp. nov.**
MycoBank No: 861118
Figs 16, 17

**Typification.** CHINA • Yunnan Province: Diqing, Weixi County, Weideng Town, Fuchuan Village, GPS coordinates 27°17'N, 99°16'E, altitude 1700 m asl., on the fallen angiosperm branch, leg. C.L. Zhao, 12 October 2023, CLZhao 34242 (SWFC 00034242), GenBank: ITS = PV829552, nLSU = PV810101.

**Etymology.** *laceratum* (Lat.): refers to the lacerate hymenial surface of the type specimens.

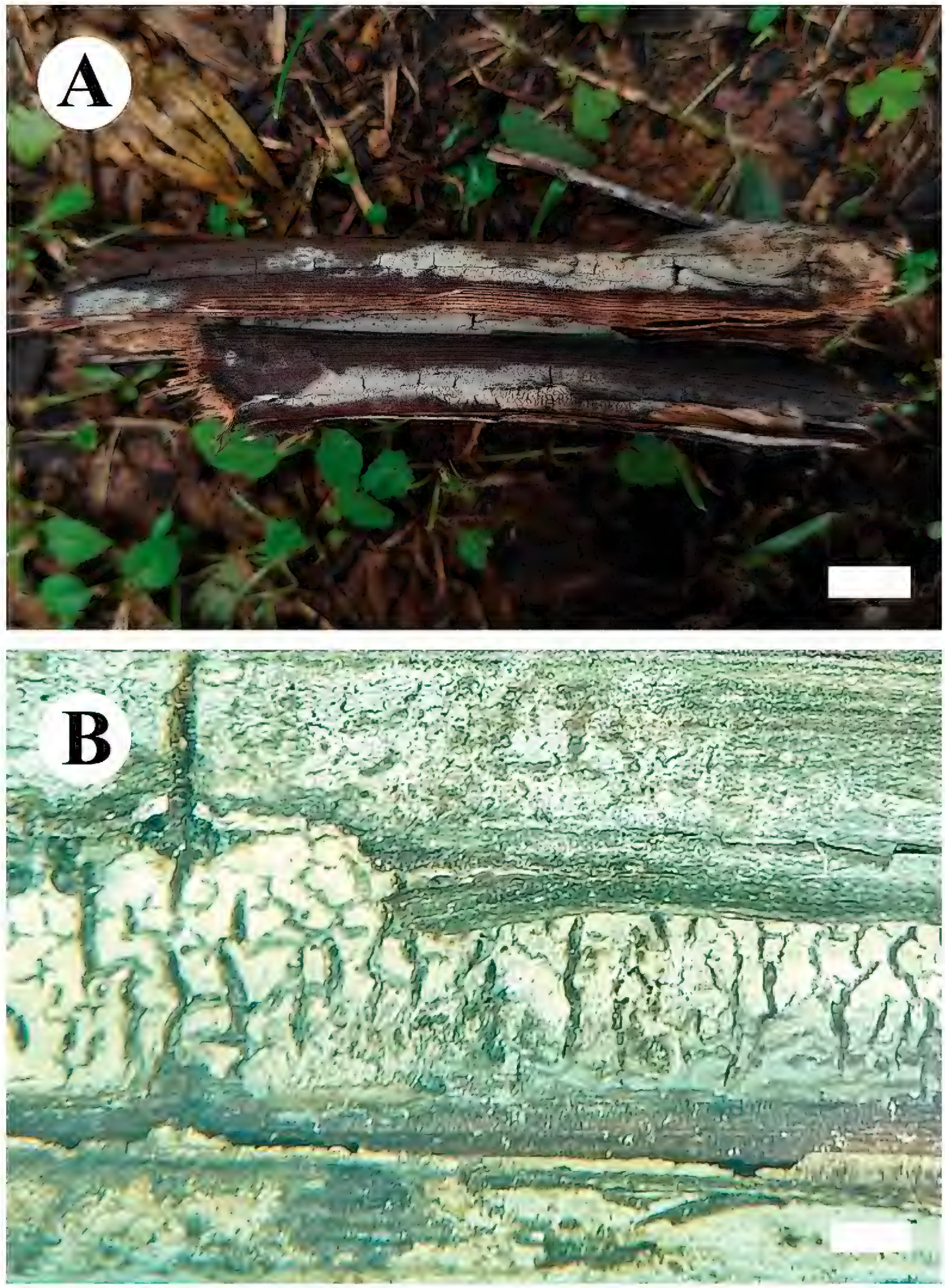


**Figure 16.** Basidiomata of *Hyphoderma laceratum* (holotype CLZhao 34242). Scale bars: 1 cm (**A**); 1 mm (**B**).

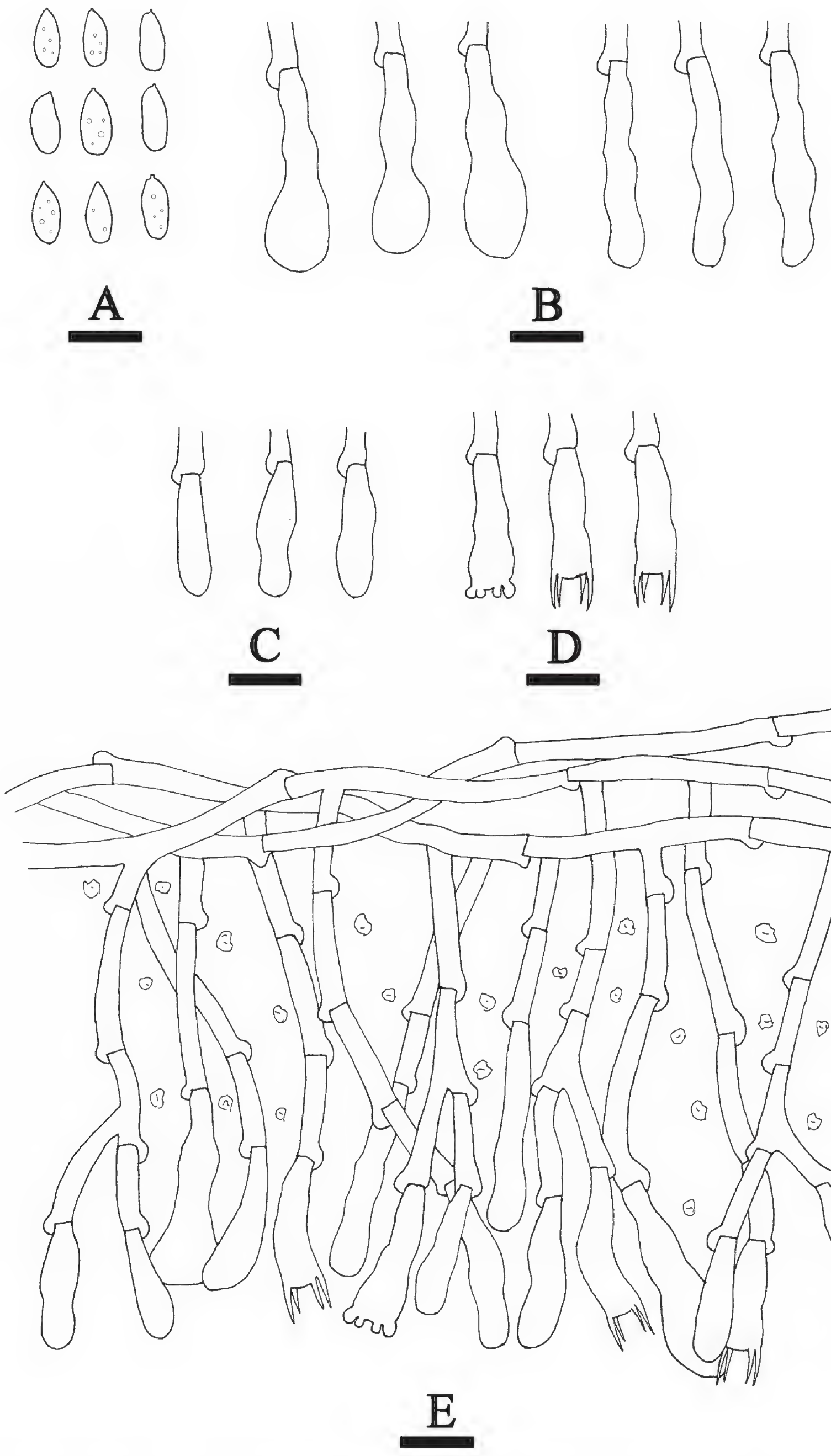


**Figure 17.** Microscopic structures of *Hyphoderma laceratum* (holotype CLZhao 34242). **A.** Basidiospores; **B.** Cystidia; **C.** Basidioles; **D.** Basidia; **E.** Part of a vertical section of the hymenium. Scale bars: 10 μm (**A–E**).

**Description.** ***Basidiomata*.** Annual, resupinate, adnate, membranaceous, without odor or taste when fresh, up to 10.5 cm long, 2.5 cm wide, and 150 μm thick. Hymenial surface smooth, white to cream when fresh, becoming cream when dry. Sterile margin narrow, white, up to 1 mm.

***Hyphal system*.** Monomitic; generative hyphae with clamp connections, colorless, thin-walled, branched, interwoven, 2.5–3.3 μm in diameter, IKI–, CB–, tissues unchanged in KOH.

***Hymenium*.** Cystidia, two types: (1) Clavate, colorless, thin-walled, smooth, 27–29 × 6.5–8 μm; (2) Capitate, colorless, thin-walled, smooth, 26–30 × 7.5–8.5 μm. Basidia subcylindrical, thin-walled, smooth, slightly flexuous, with four sterigmata and a simple septum at the base, 18–20.5 × 5–7 μm; basidioles similar to basidia in shape but slightly smaller.

***Spores*.** Basidiospores sub-ellipsoid, colorless, thin-walled, smooth, with guttulate, IKI–, CB–, (6–)6.5–9 × (2.5–)3–4(–4.5) μm, L = 7.72 μm, W = 3.49 μm, Q = 2.18–2.35 (n = 330/11).

**Additional specimens examined (paratypes).** China • Yunnan Province: Diqing, Weixi County, Weideng Town, Fuchuan Village, GPS coordinates 27°17'N, 99°16'E, altitude 1700 m asl., on the fallen angiosperm branch, leg. C.L. Zhao, 12 October 2023, CLZhao 34163 (SWFC 00034163), CLZhao 34138 (SWFC 00034138); • Zhonglu Town, GPS coordinates 27°17'N, 99°16'E, altitude 1811 m asl., on the fallen angiosperm branch, leg. C.L. Zhao, 15 October 2023, CLZhao 34961 (SWFC 00034961), CLZhao 35040 (SWFC 00035040), CLZhao 34718 (SWFC 00034718), CLZhao 34672 (SWFC 00034672), CLZhao 34958 (SWFC 00034958); • Qujing, Zhanyi District, Lingjiao Town, Xiajia Village, GPS coordinates 25°8'N, 103°6'E, altitude 2040 m asl., on the fallen angiosperm branch, leg. C.L. Zhao, 6 March 2023, CLZhao 27226 (SWFC 00027226); • Dehong, Yingjiang County, Tongbiguan Provincial Nature Reserve, GPS coordinates 24°30'N, 97°30'E, altitude 1006 m asl., on the fallen angiosperm branch, leg. C.L. Zhao, 19 July 2023, CLZhao 30414 (SWFC 00030414), CLZhao 30552 (SWFC 00030552).

**Notes.** In the phylogenetic analysis, *Hyphoderma laceratum* (CLZhao 34958, CLZhao 34672, CLZhao 34961, CLZhao 34242) formed a closely related sister relationship with *H. marginatum* (CLZhao 3404), with 99% ML bootstrap support and a 0.99 BYPP value. However, morphologically, *H. marginatum* differs from *H. laceratum* by having a cream hymenial surface and longer basidia (21–31.5 × 5–7 μm vs. 18–20.5 × 5–7 μm; Duan et al. 2023). Morphologically, *H. laceratum* is similar to *H. niveomarginatum* by having a cream hymenial surface (Yang et al. 2023). Further, *H. niveomarginatum* is distinguished from *H. laceratum* by its moniliform cystidia (Yang et al. 2023). Based on these morphological differences and phylogenetic analysis, we propose it as a new species, *Hyphoderma laceratum*.

## Discussion and conclusion

Many recently described wood-decaying fungal taxa have been reported from subtropical and tropical regions, and the genus *Hyphoderma* represents one of the most rapidly expanding groups in these areas (Nilsson et al. 2003; Wu et al. 2010; Martín et al. 2018; Guan and Zhao 2021a, b). Molecular systematics and taxonomy are essential for resolving diversity within *Hyphoderma* because species in this genus exhibit substantial variation in basidiomata morphology, including farinaceous,

coriaceous, and membranaceous forms, as well as hymenophore types ranging from smooth to grandinioid (Guan et al. 2023; Su et al. 2024; Li et al. 2025; Yang et al. 2025b). Despite this variation, the hymenial surface predominantly ranges from cream to whitish (Yurchenko and Wu 2014a, b; Guan et al. 2023; Wang et al. 2025). The morphological delineation of *Hyphoderma* species is challenging, and continuous descriptions of new taxa further reduce the diagnostic value of the limited morphological characteristics available for distinguishing species within each morpho-ecological group (Yang et al. 2025b). In the present study, we described five new species, viz., *H. alboarachnum*, *H. bambusinum*, *H. fulgens*, *H. grandineum*, and *H. laceratum*. These taxa represent distinct hymenophore types and highlight the necessity of integrative taxonomy for accurate species identification.

Wood-decaying fungi occupy a broad range of substrates, including living trees, decorticated wood of dead branches and trunks, and processed wood materials (Dai et al. 2015; Cui et al. 2019; Zhao et al. 2023; Zhang et al. 2023; He et al. 2024; Hyde et al. 2024; Luo et al. 2024; Deng et al. 2025; Yang et al. 2025a). Recent biogeographical studies, particularly in Polyporaceae and Hymenochaetaceae, have substantially improved our understanding of diversification patterns among wood-decaying fungi (Yang et al. 2023; Zhao et al. 2025). Consistent with these findings, our results show that the geographic distribution of *Hyphoderma* follows a distinct and well-structured biogeographical pattern, similar to that observed in other major groups of wood-decaying fungi (Song and Cui 2017; Yang et al. 2023).

Molecular dating analyses have provided important insights into the evolution of wood-decaying fungi (Zhao et al. 2025). According to our divergence-time estimates based on ITS and nLSU sequence datasets, *Hyphoderma* likely originated during the Cretaceous period. The mean stem age is 117.76 Mya (95% HPD = 92.38–147.74 Mya), with strong support (PP = 1.0). This deep evolutionary origin is consistent with the long-term ecological continuity of Cretaceous forest ecosystems (Martín et al. 2018; Cui et al. 2025). Our biogeographical reconstruction further suggests that *Hyphoderma* most likely originated in Asia, a recognized global biodiversity hotspot (Cui et al. 2025). Dispersal between East Asia and North America may have occurred through Beringia (Cui et al. 2025; Zhao et al. 2025). In contrast, later vicariance events, such as the opening of the Bering Strait, probably restricted gene flow between the Old and New Worlds and contributed to the present distribution of the genus (Hibbett 2001; Cai et al. 2014; Zhao et al. 2025).

In summary, by combining extensive field collections, detailed morphological observations, and multi-locus phylogenetic analyses, we reconstructed the evolutionary relationships within *Hyphoderma* and uncovered five previously unknown species. Our divergence-time and biogeographical analyses provide a refined understanding of the evolutionary origin and historical distribution of the genus, thereby contributing valuable insights into the broader evolutionary history of wood-decaying fungi. The present study fills knowledge gaps regarding wood-inhabiting fungi by reporting new taxa and providing detailed morphological descriptions and phylogenetic analyses while contributing to the enrichment of fungal diversity in Asia.

## Additional information

### Conflict of interest

The authors have declared that no competing interests exist.

## Ethical statement

No ethical statement was reported.

## Use of AI

No use of AI was reported.

## Funding

The research was supported by the Forestry and Grass Science and Technology Innovation Joint Project of Yunnan Province (Project No. 202404CB090008), the Forestry Innovation Programs of Southwest Forestry University (Grant No. LXXK-2025D20), Modern Industry School of Edible-fungi, Southwest Forestry University (SYJ25), Comprehensive Scientific Investigation of Biluo Snow Mountain in Diqing Prefecture (996323139), and the High-level Talents Program of Yunnan Province (YNQR-QNRC-2018-111).

## Author contributions

Contribution, CZ and WL; methodology, CZ; software, CZ and WL; validation, CZ; formal analysis, CZ and WL; investigation, CZ and WL; resources, CZ; writing—original draft preparation, WL, HW, XW, LX, WK, SN, and CZ; writing—review and editing, CZ and WL; visualization, CZ; supervision, CZ; project administration, CZ; funding acquisition, CZ. All authors have read and agreed to the published version of the manuscript.

## Author ORCIDs

Wen Li https://orcid.org/0009-0005-1394-4945
Haijiao Wang https://orcid.org/0009-0008-7690-2576
Xiyan Wang https://orcid.org/0009-0006-9978-1901
Xiuhe Liao https://orcid.org/0009-0005-8288-0340
Kaisheng Wang https://orcid.org/0009-0007-4840-816X
Wijesinghe Arachchige Subodini Nuwanthika https://orcid.org/0000-0002-5625-9578
Changlin Zhao https://orcid.org/0000-0002-8668-1075

## Data availability

All of the data that support the findings of this study are available in the main text.

## References

Bernicchia A, Gorjón SP (2010) Fungi Europaei 12: Corticiaceae s.l. Edizioni Candusso, Lomazzo, 1–1007.

Boonmee S, Wanasinghe DN, Calabon MS, Huanraluek N, Chandrasiri SKU, Jones GEB, Rossi W, Leonardi M, Singh SK, Rana S, Singh PN, Maurya DK, Lagashetti AC, Choudhary D, Dai YC, Zhao CL, Mu YH, Yuan HS, He SH, Phookamsak R, Jiang HB, Martín MP, DueñasM, Tellería MT, Kałucka IL, Jagodziński AM, Liimatainen K, Pereira DS, Phillips AJL, Suwannarach N, Kumla J, Khuna S, Lumyong S, Potter TB, Shivas RG, Sparks AH, VaghefiN, Abdel-Wahab MA, Abdel-Aziz FA, Li GJ, Lin WF, Singh U, Bhatt RP, Lee HB, NguyenTTT, Kirk PM, Dutta AK, Acharya K, Sarma VV, Niranjan M, Rajeshkumar KC, AshtekarN, Lad S, Wijayawardene NN, Bhat DJ, Xu RJ, Wijesinghe SN, Shen HW, Luo ZL, Zhang JY, Sysouphanthong P, Thongklang N, Bao DF, Aluthmuhandiram JVS, AbdollahzadehJ, Javadi A, Dovana F, Usman M, Khalid AN, Dissanayake AJ, Telagathoti A, Probst M, Peintner U, Garrido-Benavent I, Bóna L, Merényi Z, Boros L, Zoltán B, Stielow JB, Jiang N, Tian CM, Shams E, Dehghanizadeh F, Pordel A, Javan-Nikkhah M, Denchev

TT, DenchevCM, Kemler M, Begerow D, Deng CY, Harrower E, Bozorov T, Kholmuradova T, GafforovY, Abdurazakov A, Xu JC, Mortimer PE, Ren GC, Jeewon R, Maharachchikumbura SSN, Phukhamsakda C, Mapook A, Hyde KD (2021) Fungal diversity notes 1387–1511: Taxonomic and phylogenetic contributions on genera and species of fungal taxa. Fungal Diversity 111: 1–335. https://doi.org/10.1007/s13225-021-00489-3

Caboň M, Li GJ, Saba M, Kolařík M, Jančovičová S, Khalid AN, Moreau PA, Wen HA, Pfister DH, Adamčík S (2019) Phylogenetic study documents different speciation mechanisms within the *Russula globispora* lineage in boreal and arctic environments of the Northern Hemisphere. IMA Fungus 10: 5. https://doi.org/10.1186/s43008-019-0003-9

Cai Q, Tulloss RE, Tang LP, Tolgor B, Zhang P, Chen ZH, Yang ZL (2014) Multi-locus phylogeny of lethal amanitas: Implications for species diversity and historical biogeography. BMC Evolutionary Biology 14: 143. https://doi.org/10.1186/1471-2148-14-143

Cho Y, Kim D, Lee Y, Jeong J, Hussain S, Lim YW (2023) Validation of *Fuscoporia* (Hymenochaetales, Basidiomycota) ITS sequences and five new species based on multi-marker phylogenetic and morphological analyses. IMA Fungus 14: 12. https://doi.org/10.1186/s43008-023-00117-6

Cui BK, Li HJ, Ji X, Zhou JL, Song J, Si J, Yang ZL, Dai YC (2019) Species diversity, taxonomy and phylogeny of Polyporaceae (Basidiomycota) in China. Fungal Diversity 97: 137–392. https://doi.org/10.1007/s13225-019-00427-4

Cui YJ, Wang CG, Dai YC, Liu S, Ren YH, Schultes NP, Kaishian PO, Paine E, Yuan Y, Li DW, Zhao H (2025) Phylogeny, divergence times, and biogeography of the phytopathogenic fungal genus *Phaeolus* (Basidiomycota, Polyporales). Journal of Systematics and Evolution 00: 1–15. https://doi.org/10.1111/jse.13187

Dai YC (2012) Polypore diversity in China with an annotated checklist of Chinese polypores. Mycoscience 53: 49–80. https://doi.org/10.1007/s10267-011-0134-3

Dai YC, Cui BK, Si J, He SH, Hyde KD, Yuan HS, Liu XY (2015) Dynamics of the worldwide number of fungi with emphasis on fungal diversity in China. Mycological Progress 14: 1–9. https://doi.org/10.13346/j.mycosystema.210036

Deng YL, Chen M, Liu LF, Li QZ, Zhang SC, Yuan HS, Zhao CL (2025) Morphological and molecular analyses revealed four new wood-inhabiting fungal species (Hymenochaetales, Basidiomycota) from Yunnan. MycoKeys 117: 29–66. https://doi.org/10.3897/mycokeys.117.146236

Dong JH, Yuan Q, Luo YX, Zhang XC, Dai YF, Zhou Q, Liu XF, Deng YL, Zhou HM, Muhammad A, Zhao CL (2024) Species diversity, taxonomy, molecular systematics and divergence time of wood-inhabiting fungi in Yunnan-Guizhou Plateau, Asia. Mycosphere: Journal of Fungal Biology 15: 1110–1293. https://doi.org/10.5943/mycosphere/15/1/10

Dong JH, Chen ML, Chen M, Li Q, Zhu YJ, Zhang XC, Zhou CQ, Li W, Muhammad A, Zhou HM, Jabeen S, Zhao CL (2025) Notes, outline, taxonomy and phylogeny of wood-inhabiting Agaricales. Mycosphere: Journal of Fungal Biology 16: 2599–2711. https://doi.org/10.5943/mycosphere/16/1/16

Donk MA (1957) Notes on resupinate Hymenomycetes IV. Fungus 27: 1–29.

Duan ZY, Guan QX, Luo KY, Zhao CL (2023) Morphological and molecular identification of three new resupinate species of *Hyphoderma* (Hyphodermataceae, Agaricomycetes) from East Asia. Phytotaxa 599: 1–19. https://doi.org/10.11646/phytotaxa.599.1.1

Felsenstein J (1985) Confidence intervals on phylogenetics: An approach using bootstrap. Evolution; International Journal of Organic Evolution 39: 783–791. https://doi.org/10.1111/j.1558-5646.1985.tb00420.x

Floudas D (2021) Chapter Two - Evolution of lignin decomposition systems in fungi. Advances in Botanical Research 99: 37–76. https://doi.org/10.1016/bs.abr.2021.05.003

Floudas D, Binder M, Riley R, Barry K, Blanchette RA, Henrissat B, Martínez AT, Otillar R, Spatafora JW, Yadav JS, Aerts A, Benoit I, Boyd A, Carlson A, Copeland A, Coutinho PM, de Vries RP, Ferreira P, Findley K, Foster B, Gaskell J, Glotzer D, Górecki P, Heitman J, Hesse C, Hori C, Igarashi K, Jurgen JA, Kallen N, Kersten P, Kohler A, Kües U, Kumar TKA, Kuo A, LaButti K, Larrondo LF, Lindquist E, Ling A, Lombard V, Lucas S, Lundell T, Martin R, McLaughlin DJ, Morgenstern I, Morin E, Murat C, Nagy LG, Nolan M, Ohm RA, Patyshakuliyeva A, Rokas A, Ruiz Dueñas FJ, Sabat G, Salamov A, Samejima M, Schmutz J, Slot JC, John FS, Stenlid J, Sun H, Sun S, Syed K, Tsang A, Wiebenga A, Young D, Pisabarro A, Eastwood DC, Martin F, Cullen D, Grigoriev IV, Hibbett DS (2012) The Paleozoic origin of enzymatic lignin decomposition reconstructed from 31 fungal genomes. Science 336: 1715–1719. https://doi.org/10.1126/science.1221748

Floudas D, Hibbett DS (2015) Revisiting the taxonomy of Phanerochaete (Polyporales, Basidiomycota) using a four gene dataset and extensive ITS sampling. Fungal Biology 119(8): 679–719. https://doi.org/10.1016/j.funbio.2015.04.003

Guan QX, Zhao CL (2021a) Taxonomy and phylogeny of the wood-inhabiting fungal genus *Hyphoderma* with descriptions of three new species from East Asia. Journal of Fungi (Basel, Switzerland) 7: 308. https://doi.org/10.3390/jof7040308

Guan QX, Zhao CL (2021b) Two new corticioid species: *Hyphoderma sinense* and *H. floccosum* spp. nov. (Hyphodermataceae, Polyporales) from southern China. Mycosystema 40: 447–461. https://doi.org/10.13346/j.mycosystema.200382

Guan QX, Li YF, Zhao CL (2021) Morphological and phylogenetic evidence for recognition of two new species of *Hyphoderma* (Basidiomycota) from southern China, with a key to all Chinese *Hyphoderma*. MycoKeys 83: 145–160. https://doi.org/10.3897/mycokeys.83.69909

Guan QX, Huang J, Huang J, Zhao CL (2023) Five new species of Schizoporaceae (Basidiomycota, Hymenochaetales) from East Asia. MycoKeys 96: 25–56. https://doi.org/10.3897/mycokeys.96.99327

Hawksworth DL, Lücking R (2017) Fungal diversity revisited: 2.2 to 3.8 million species. Microbiology Spectrum 5: 1–17. https://doi.org/10.1128/microbiolspec.FUNK-0052-2016

He MQ, Zhao RL, Hyde KD, Begerow D, Kemler M, Yurkov A (2019) Notes, outline and divergence times of Basidiomycota. Fungal Diversity 99: 105–367. https://doi.org/10.1007/s13225-019-00435-4

He MQ, Cao B, Liu F, Boekhout T, Denchev TT, Power N, Denchev CM, Kemler M, Gorjón SP, Begerow D, Valenzuela R, Davoodian N, Niskanen T, Vizzini A, Redhead SA, Ramírez-Cruz V, Papp V, Dudka VA, Dutta AK, García-Sandoval R, Liu XZ, Kijpornyongpan T, Savchenko A, Tedersoo L, Theelen B, Trierveiler-Pereira L, Wu F, Zamora JC, Zeng XY, Zhou LW, Liu SL, Ghobad-Nejhad M, Giachini AJ, Li GJ, Kakishima M, Olariaga I, Haelewaters D, Sulistyo B, Sugiyama J, Svantesson S, Yurkov A, Alvarado P, Antonín V, da Silva AF, Druzhinina I, Gibertoni TB, Guzmán Davalos L, Justo A, Karunarathna SC, Galappaththi MCA, Toome-Heller M, Hosoya T, Liimatainen K, Márquez R, Mešić A, Moncalvo JM, Nagy LC, Varga T, Orihara T, Raymundo T, Salcedo I, Silva-Filho AGS, Tkalčec Z, Wartchow F, Zhao CL, Bau T, Cabarroi-Hernández M, CortésPérez A, Decock C, De Lange R, Weiss M, Menolli N, Nilsson RH, Fan YG, Verbeken A, Gaforov Y, Meiras-Ottoni A, Mendes-Alvarenga RL, Zeng NK, Wu Q, Hyde KD, Kirk PM, Zhao RL (2024) Phylogenomics, divergence times and notes of orders in Basidiomycota. Fungal Diversity 126: 1–280. https://doi.org/10.1007/s13225-024-00535-W

Hibbett DS (2001) Shiitake mushrooms and molecular clocks: Historical biogeography of *Lentinula*. Journal of Biogeography 28: 231–241. https://doi.org/10.1046/j.1365-2699.2001.00528.x

Hibbett D, Nagy LG, Nilsson RH (2025) Fungal diversity, evolution, and classification. Current Biology 35(11): R427–R526. https://doi.org/10.1016/j.cub.2025.01.053

Hyde KD, Noorabadi MT, Thiyagaraja V, He MQ, Johnston PR, Wijesinghe SN, Armand A, Biketova AY, Chethana KWT, Erdoğdu M, Ge ZW, Groenewald JZ, Hongsanan S, Kušan I, Leontyev DV, Li DW, Lin CG, Liu NG, Maharachchikumbura SSN, Matočec N, May TW, McKenzie EHC, Mešić A, Perera RH, Phukhamsakda C, Piątek M, Samarakoon MC, Selcuk F, Senanayake IC, Tanney JB, Tian Q, Vizzini A, Wanasinghe DN, Wannasawang N, Wijayawardene NN, Zhao RL, Abdel-Wahab MA, Abdollahzadeh J, Abeywickrama PD, Abhinav, Absalan S, Acharya K, Afshari N, Afshan NS, Afzalinia S, Ahmadpour SA, Akulov O, Alizadeh A, Alizadeh M, Al-Sadi AM, Alves A, AlvesVCS, Alves-Silva G, Antonín V, Aouali S, Aptroot A, Apurillo CCS, Arias RM, Asgari B, Asghari R, Assis DMA, Assyov B, Atienza V, Aumentado HDR, Avasthi S, Azevedo E, Bakhshi M, Bao DF, Baral HO, Barata M, Barbosa KD, Barbosa RN, Barbosa FR, Baroncelli R, Barreto GG, Baschien C, Bennett RM, Bera I, Bezerra JDP, Bhunjun CS, Bianchinotti MV, Błaszkowski J, Boekhout T, Bonito GM, Boonmee S, Boonyuen N, BortnikovFM, Bregant C, Bundhun D, Burgaud G, Buyck B, Caeiro MF, Cabarroi-Hernández M, Cai M Feng, Cai L, Calabon MS, Calaça FJS, Callalli M, Câmara MPS, Cano-Lira J, Cao B, Carlavilla JR, Carvalho A, Carvalho TG, Castañeda-Ruiz RF, Catania MDV, Cazabonne J, Cedeño-Sanchez M, Chaharmiri-Dokhaharani S, Chaiwan N, Chakraborty N, Cheewankoon R, Chen C, Chen J, Chen Q, Chen YP, Chinaglia S, Coelho-NascimentoCC, Coleine C, CostaRezende DH, Cortés-Pérez A, Crouch JA, Crous PW, Cruz RHSF, Czachura P, Damm U, Darmostuk V, Daroodi Z, Das K, Das K, Davoodian N, DavydovEA, da Silva GA, da Silva IR, da Silva RMF, da Silva Santos AC, Dai DQ, Dai YC, de GrootMichiel D, De Kesel A, De Lange R, de Medeiros EV, de Souza CFA, de Souza FA, delaCruz TEE, Decock C, Delgado G, Denchev CM, Denchev TT, Deng YL, Dentinger BTM, Devadatha B, Dianese JC, Dima B, Doilom M, Dissanayake AJ, Dissanayake DMLS, Dissanayake LS, Diniz AG, Dolatabadi S, Dong JH, Dong W, Dong ZY, Drechsler-Santos ER, Druzhinina IS, Du TY, Dubey MK, Dutta AK, Elliott TF, Elshahed MS, Egidi E, Eisvand P, Fan L, Fan X, Fan XL, Fedosova AG, Ferro LO, Fiuza PO, Flakus AW, Fonseca EO, Fryar SC, Gabaldón T, Gajanayake AJ, Gannibal PB, Gao F, GarcíaSánchez D, García-Sandoval R, Garrido-Benavent I, Garzoli L, Gasca-Pineda J, Gautam AK, GenéJ, Ghobad-Nejhad M, Ghosh A, Giachini AJ, Gibertoni TB, Gentekaki E, GmoshinskiyVI, GóesNeto A, Gomdola D, Gorjón SP, Goto BT, Granados-Montero MM, Griffith GW, Groenewald M, Grossart H-P, Gu ZR, Gueidan C, Gunarathne A, Gunaseelan S, GuoSL, Gusmão LFP, Gutierrez AC, Guzmán-Dávalos L, Haelewaters D, Haituk H, HallingRE, He SC, Heredia G, HernándezRestrepo M, Hosoya T, Hoog SD, Horak E, Hou CL, Houbraken J, Htet ZH, Huang SK, Huang WJ, Hurdeal VG, Hustad VP, Inácio CA, Janik P, Jayalal RGU, Jayasiri SC, Jayawardena RS, Jeewon R, Jerônimo GH, Jin J, JonesEBG, Joshi Y, Jurjević Ž, Justo A, Kakishima M, Kaliyaperumal M, Kang GP, Kang JC, Karimi O, Karunarathna SC, Karpov SA, Kezo K, Khalid AN, Khan MK, Khuna S, KhyajuS, Kirchmair M, Klawonn I, Kraisitudomsook N, Kukwa M, Kularathnage ND, KumarS, Lachance MA, Lado C, Latha KPD, Lee HB, Leonardi M, Lestari AS, Li C, Li H, Li J, Li Q, Li Y, Li YC, Li YX, Liao CF, Lima JLR, Lima JMS, Lima NB, Lin L, Linaldeddu BT, inn MM, Liu F, Liu JK, Liu JW, Liu S, Liu SL, Liu XF, Liu XY, Longcore JE, Luangharn T, uangsa-ard JJ, Lu L, Lu YZ, Lumbsch HT, Luo L, Luo M, Luo ZL, Ma J, Madagammana AD, Madhushan A, Madrid H, Magurno F, Magyar D, Mahadevakumar S, Malosso E, Malysh JM, Mamarabadi M, Manawasinghe IS, Manfrino RG, Manimohan P, MaoN, Mapook A, Marchese P, Marasinghe DS, Mardones M, Marin-Felix Y, Masigol H, ehrabi M, MehrabiKoushki M, Meiras-Ottoni A de, Melo RFR, Mendes-Alvarenga RL, Mendieta S, Meng QF, Menkis A, Menolli Jr N, Mikšík M, Miller SL, Moncada B, Moncalvo

JM, Monteiro JS, Monteiro M, Mora-Montes HM, Moroz EL, Moura JC, Muhammad U, Mukhopadhyay S, Nagy GL, Najam ul Sehar A, Najafiniya M, Nanayakkara CM, Naseer A, Nascimento ECR, Nascimento SS, Neuhauser S, Neves MA, Niazi AR, Nie Yong, Nilsson RH, Nogueira PTS, Novozhilov YK, Noordeloos M, NorphanphounC, Nuñez Otaño N, O'Donnell RP, Oehl F, Oliveira JA, Oliveira Junior I, Oliveira NVL, Oliveira PHF, Orihara T, Oset M, Pang KL, Papp V, Pathirana LS, Peintner U, Pem D, Pereira OL, Pérez-Moreno J, Pérez-Ortega S, Péter G, Pires-Zottarelli CLA, Phonemany M, Phongeun S, Pošta A, Prazeres JFSA, Quan Y, Quandt CA, Queiroz MB, RadekR, Rahnama K, Raj KNA, Rajeshkumar KC, Rajwar Soumyadeep, Ralaiveloarisoa AB, Rämä T, Ramírez-Cruz V, Rambold G, Rathnayaka AR, Raza M, Ren GC, Rinaldi AC, Rivas-Ferreiro M, Robledo GL, Ronikier A, Rossi W, Rusevska K, Ryberg M, Safi A, Salimi F, Salvador-Montoya CA, Samant B, Samaradiwakara NP, Sánchez-Castro I, Sandoval-Denis M, Santiago ALCMA, Santos ACDS, Santos LA dos, Sarma VV, Sarwar S, Savchenko A, Savchenko K, Saxena RK, Schoutteten N, Selbmann L, Ševčíková H, Sharma A, Shen HW, Shen YM, Shu YX, Silva HF, Silva-Filho AGS, Silva VSH, Simmons DR, Singh R, Sir EB, Sohrabi M, Souza FA, Souza-Motta CM, Sriindrasutdhi V, Sruthi OP, Stadler M, Stemler J, Stephenson SL, Stoyneva-Gaertner MP, Strassert JFH, Stryjak-Bogacka M, Su H, Sun YR, Svantesson S, Sysouphanthong P, Takamatsu S, Tan TH, Tanaka K, Tang C, Tang X, Taylor JE, Taylor PWJ, Tennakoon DS, Thakshila SAD, Thambugala KM, Thamodini GK, Thilanga D, Thines M, Tiago PV, Tian XG, Tian WH, Tibpromma S, Tkalčec Z, Tokarev YS, Tomšovský M, Torruella G, Tsurykau A, Udayanga D, Ulukapı M, Untereiner WA, Usman M, Uzunov BA, Vadthanarat S, Valenzuela R, Van den Wyngaert S, Van Vooren N, Velez P, Verma RK, Vieira LC, Vieira WAS, Vinzelj JM, Tang AMC, Walker A, Walker AK, Wang QM, Wang Y, Wang XY, Wang ZY, Wannathes N, Wartchow F, Weerakoon G, Wei DP, Wei X, White JF, Wijesundara DSA, Wisitrassameewong K, Worobiec G, Wu HX, Wu N, Xiong YR, Xu B, Xu JP, Xu R, Xu RF, Xu RJ, Yadav S, Yakovchenko LS, Yang HD, Yang X, Yang YH, Yang Y, Yang YY, Yoshioka R, Youssef Noha H, Yu FM, Yu ZF, Yuan LL, Yuan Q, Zabin DA, Zamora JC, Zapata CV, Zare R, Zeng M, Zeng XY, Zhang JF, Zhang JY, Zhang S, Zhang XC, Zhao CL, Zhao H, Zhao Q, Zhao H, Zhao HJ, Zhou HM, Zhu XY, Zmitrovich IV, Zucconi L, Zvyagina E (2024) The 2024 Outline of fungi and fungus-like taxa. Mycosphere 15: 5146–6239. https://doi.org/10.5943/mycosphere/15/1/25

Justo A, Miettinen O, Floudas D, Ortiz-Santana B, Sjökvist E, Lindner D, Nakasone K, Niemelä T, Larsson KH, Ryvarden L, Hibbett DS (2017) A revised family-level classification of the Polyporales (Basidiomycota). Fungal Biology 121: 798–824. https://doi.org/10.1016/j.funbio.2017.05.010

Katoh K, Rozewicki J, Yamada KD (2019) MAFFT online service: Multiple sequence alignment, interactive sequence choice and visualization. Briefings in Bioinformatics 20: 1160–1166. https://doi.org/10.1093/bib/bbx108

Kirk PM, Cannon PF, Minger DW, Stalpers JA (2008) Dictionary of the Fungi, 10th ed. Wallingford, UK, 1–771.

Larsson KH (2007) Re-thinking the classification of corticioid fungi. Mycological Research 111: 1040–1063. https://doi.org/10.1016/j.mycres.2007.08.001

Larsson A (2014) AliView: A fast and lightweight alignment viewer and editor for large data sets. Bioinformatics (Oxford, England) 30: 3276–3278. https://doi.org/10.1093/bioinformatics/btu531

Li W, Wang XY, Chen DX, Zhang SC, Li YC, Zhao CL, Zhan ZY (2025) Molecular phylogeny and morphology reveal a new wood-inhabiting fungus *Hyphoderma cinereofuscum* (Polyporales, Basidiomycota), from southwest China. Phytotaxa 683: 106–118. https://doi.org/10.11646/phytotaxa.683.2.2

Luo KY, Su JQ, Zhao CL (2024) Morphological and molecular identification for four new wood-inhabiting species of *Trechispora* (Basidiomycota) from China. MycoKeys 105: 155–178. https://doi.org/10.3897/mycokeys.105.120438

Ma X, Huang RX, Zhang Y, Zhao CL (2021) *Hyphoderma fissuratum* and *H. mopanshanense* spp. nov. (Polyporales) from southern China. Mycoscience 62: 36–41. https://doi.org/10.47371/mycosci.2020.08.004

Mao WL, Wu YD, Liu HG, Yuan Y, Dai YC (2023) A contribution to *Porogramme* (Polyporaceae, Agaricomycetes) and related genera.

Martín MP, Zhang LF, Fernández-López J, Dueñas M, Rodríguez-Armas JL, Beltrán-Tejera E, Tellería MT (2018) *Hyphoderma paramacaronesicum* sp. nov. (Meruliaceae, Polyporales, Basidiomycota), a cryptic lineage to *H. macaronesicum*. Fungal Systematics and Evolution 2: 57–68. https://doi.org/10.3114/fuse.2018.02.05

Miller MA, Pfeiffer W, Schwartz T (2012) The CIPRES science gateway: Enabling high–impact science for phylogenetics researchers with limited resources. Association for Computing Machinery 39: 1–8. https://doi.org/10.1145/2335755.2335836

Nagy LG, Branco S, Floudas D, Hibbett DS, Lofgren L, Martin F, Merényi Z, Plett JM, Pringle A, Varga T (2025) The biodiversity, genomics, ecology and evolution of mushroom-forming fungi. Nature Reviews Biodiversity 2: 24–39. https://doi.org/10.1038/s44358-025-00107-z

Nakasone KK (2008) Type studies of corticioid Hymenomycetes described by Bresadola. Cryptogamie. Mycologie: 29.

Nilsson RH, Hallenberg N, Nordén B, Maekawa N, Wu SH (2003) Phylogeography of *Hyphoderma setigerum* (Basidiomycota) in the northern hemisphere. Mycological Research 107: 645–652. https://doi.org/10.1017/S0953756203007925

Niskanen T, Lücking R, Dahlberg A, Gaya E, Suz LM, Mikryukov V, Liimatainen K, Druzhinina I, Westrip JRS, Mueller GM, Martins-Cunha K, Kirk P, Tedersoo L, Antonelli A (2023) Pushing the frontiers of biodiversity research: Unveiling the global diversity, distribution, and conservation of fungi. Annual Review of Environment and Resources 48(1): 149–176. https://doi.org/10.1146/annurev-environ-112621-090937

Nylander JAA (2004) MrModeltest v2. Program Distributed by the Author, Evolutionary Biology Centre, Uppsala University, Uppsala, Sweden.

Pagin-Cláudio F, Gugliotta AM (2024) Six new records of polypores (Agaricomycetes, Basidiomycota) from Southeast Brazil (Atlantic Forest) and perspectives in basic mycological research. Rodriguésia 76: e00672024. https://doi.org/10.1590/2175-7860202576010

Parmasto E (1968) Conspectus Systematis Corticiacearum 1–261.

Petersen JH (1996) Farvekort. The Danish Mycological Society's Colour-Chart. Foreningen til Svampekundskabens Fremme, Greve, Germany, 1–6

Rathnayaka AR, Tennakoon DS, Jones GE, Wanasinghe DN, Bhat DJ, Priyashantha AH, Stephenson SL, Tibpromma S, Karunarathna SC (2025) Significance of precise documentation of hosts and geospatial data of fungal collections, with an emphasis on plant-associated fungi. New Zealand Journal of Botany 63(2–3): 462–489. https://doi.org/10.1080/0028825x.2024.2381734

Ronquist F, Teslenko M, Mark PVD, Ayres DL, Darling A, Hohna S, Larget B, Liu L, Suchard MA, Huelsenbeck JP (2012) Mrbayes 3.2: Efficient bayesian phylogenetic inference and model choice across a large model space. Systematic Biology 61: 539–542. https://doi.org/10.1093/sysbio/sys029

Savinova OS, Moiseenko KV, Vavilova EA, Chulkin AM, Fedorova TV, Tyazhelova TV, Vasina DV (2019) Evolutionary relationships retween the laccase genes of Polyporales: Or-

thology-based classification of laccase isozymes and functional insight from *Trametes hirsuta*. Frontiers in Microbiology 10: 152. https://doi.org/10.3389/fmicb.2019.00152

Sayers EW, Cavanaugh M, Frisse L, Pruitt KD, Schneider VA, Underwood BA, Yankie L, Karsch-Mizrachi I (2025) GenBank 2025 update. Nucleic Acids Research 53: D56–D61. https://doi.org/10.1093/nar/gkae1114

Song J, Cui BK (2017) Phylogeny, divergence time and historical biogeography of *Laetiporus* (Basidiomycota, Polyporales). BMC Evolutionary Biology 17: 102. https://doi.org/10.1186/s12862-017-0948-5

Spirin V, Runnel K, Vlasák J, Viner I, Barrett MD, Ryvarden L, Bernicchia A, Rivoire B, Ainsworth AM, Grebenc T, Cartabia M, Niemelä T, Larsson KH, Miettinen O (2024) The genus *Fomitopsis* (Polyporales, Basidiomycota) reconsidered. Studies in Mycology 107: 149–249. https://doi.org/10.3114/sim.2024.107.03

Su JQ, Zhang XC, Zhao CL, Zhou HM (2024) Molecular phylogeny and morphology reveal a new wood-inhabiting fungal species, *Hyphoderma guangdongense* (Polyporales, Basidiomycota), from China. Phytotaxa 661: 075–086. https://doi.org/10.11646/phytotaxa.661.1.5

Sun YF, Xing JH, He XL, Wu DM, Song CG, Liu S, Vlasák J, Gates G, Gibertoni TB, Cui BK (2022) Species diversity, systematic revision and molecular phylogeny of Ganodermataceae (Polyporales, Basidiomycota) with an emphasis on Chinese collections. Studies in Mycology 101: 287–415. https://doi.org/10.3114/sim.2022.101.05

Swofford DL (2002) *PAUP**: Phylogenetic analysis using parsimony (*and Other Methods), Version 4.0b10, Sinauer Associates: Sunderland, MA, USA.

Tellería MT, Dueñas M, Beltrán-Tejera E, Rodríguez-Armas JL, Martín MP (2012) A new species of *Hyphoderma* (Meruliaceae, Polyporales) and its discrimination from closely related taxa. Mycologia 104: 1121–1132. https://doi.org/10.3852/11-344

Varga T, Krizsán K, Földi C, Dima B, Sánchez-García M, Sánchez-Ramírez S, Szöllősi GJ, Szarkándi JG, Papp V, Albert L, Andreopoulos W, Angelini C, Antonín V, Barry KW, Bougher NL, Buchanan P, Buyck B, Bense V, Catcheside P, Chovatia M, Cooper J, Dämon W, Desjardin D, Finy P, Geml J, Haridas S, Hughes K, Justo A, Karasiński D, Kautmanova I, Kiss B, Kocsubé S, Kotiranta H, LaButti KM, Lechner BE, Liimatainen K, Lipzen A, Lukács Z, Mihaltcheva S, Morgado LN, Niskanen T, Noordeloos ME, Ohm RA, Ortiz-Santana B, Ovrebo C, Rácz N, Riley R, Savchenko A, Shiryaev A, Soop K, Spirin V, Szebenyi C, Tomšovský M, Tulloss RE, Uehling J, Grigoriev IV, Vágvölgyi C, Papp T, Martin FM, Miettinen O, Hibbett DS, Nagy LG (2019) Megaphylogeny resolves global patterns of mushroom evolution. Nature Ecology and Evolution 3: 668–678. https://doi.org/10.1038/s41559-019-0834-1

Vu D, Groenewald M, De Vries M, Gehrmann T, Stielow B, Eberhardt U, Verkley GJM (2019) Large-scale generation and analysis of filamentous fungal DNA barcodes boosts coverage for kingdom fungi and reveals thresholds for fungal species and higher taxon delimitation. Studies in Mycology 92: 135–154. https://doi.org/10.1016/j.simyco.2018.05.001

Wang XW, Liu SL, Zhou LW (2023) An updated taxonomic framework of Hymenochaetales (Agaricomycetes, Basidiomycota). Mycosphere: Journal of Fungal Biology 14: 452–496. https://doi.org/10.5943/mycosphere/14/1/6

Wang L, Zhu YG, He SY, Jabeen S, Zhao CL (2025) Additions to the coriaceous families Peniophoraceae and Stereaceae (Russulales): Six novel wood-inhabiting taxa in the genera *Conferticium*, *Gloeocystidiellum*, and *Peniophora* from southwest China. MycoKeys 115: 273–308. https://doi.org/10.3897/mycokeys.115.147044

Wu SH (1997) New species of *Hyphoderma* from Taiwan. Mycologia 89: 132–140. https://doi.org/10.1080/00275514.1997.12026764

Wu SH, Nilsson HR, Chen CT, Yu SY, Hallenberg N (2010) The white-rotting genus *Phanerochaete* is polyphyletic and distributed throughout the phleboid clade of the Polyporales (Basidiomycota). Fungal Diversity 42: 107–118. https://doi.org/10.1007/s13225-010-0031-7

Wu F, Zhou LW, Yang ZL, Bau T, Li TH, Dai YC (2019) Resource diversity of Chinese macro fungi: Edible, medicinal and poisonous species. Fungal Diversity 98: 1–76. https://doi.org/10.1007/s13225-019-00432-7

Wu F, Zhou LW, Vlasák J, Dai YC (2022) Global diversity and systematics of Hymenochaetaceae with poroid hymenophore. Fungal Diversity 113: 1–192. https://doi.org/10.21203/rs.3.rs-719853/v1

Yang Y, Jiang QQ, Li Q, Yang JW, Cha L, Cheng LJ, Yang SQ, Zhao CL, Zhou HM (2023) Molecular systematics and taxonomic analyses of three new wood-inhabiting fungi of *Hyphoderma* (Hyphodermataceae, Basidiomycota). Journal of Fungi (Basel, Switzerland) 9: 1044. https://doi.org/10.3390/jof9111044

Yang X, Duan SJ, Li M, Li DX, Yang RC, Zhang SH, Xu TM, Li W, Zhou HM, Zhao CL (2025a) A new genus and three new species of Lycoperdaceae (Agaricales) from Southern China revealed by molecular phylogenyand taxonomy. MycoKeys 118: 147–177. https://doi.org/10.3897/mycokeys.118.153703

Yang Y, Xu Y, Wang L, Jiang QQ, Su JQ, Li R, Zhou HM, Zhao CL (2025b) Multigene phylogeny of seven wood-inhabiting fungal orders in Basidiomycota, and proposal of a new genus and thirteen new species. Mycosphere: Journal of Fungal Biology 16: 245–295. https://doi.org/10.5943/mycosphere/16/1/4

Yuan Q, Zhao CL (2024) Morphology and multigene phylogeny revealed four new species of *Xylodon* (Schizoporaceae, Basidiomycota) from southern China. MycoKeys 107: 161–187. https://doi.org/10.3897/mycokeys.107.128223

Yurchenko E, Wu SH (2014a) *Hyphoderma pinicola* sp. nov. of *H. setigerum* complex (Basidiomycota) from Yunnan, China. Botanical Studies 55: 1–8. https://doi.org/10.1186/s40529-014-0071-5

Yurchenko E, Wu SH (2014b) *Hyphoderma formosanum* sp. nov. (Meruliaceae, Basidiomycota) from Taiwan. Sydowia 66: 19–23.

Yurchenko E, Wu SH (2015) *Hyphoderma moniliforme* and *H. nemorale* (Basidiomycota) newly recorded from China. Mycosphere: Journal of Fungal Biology 6: 113–121. https://doi.org/10.5943/mycosphere/6/1/11

Zhang QY, Liu HG, Papp V, Zhou M, Dai YC, Yuan Y (2023) New insights into the classification and evolution of *Favolaschia* (Agaricales, Basidiomycota) and its potential distribution, with descriptions of eight new species. Mycosphere: Journal of Fungal Biology 14: 777–814. https://doi.org/10.5943/mycosphere/14/1/10

Zhao CL, Wu ZQ (2017) *Ceriporiopsis kunmingensis* sp. nov. (Polyporales, Basidiomycota) evidenced by morphological characters and phylogenetic analysis. Mycological Progress 16: 93–100. https://doi.org/10.1007/s11557-016-1259-8

Zhao H, Nie Y, Zong TK, Wang K, Lv ML, Cui YJ, Tohtirjap A, Chen JJ, Zhao CL, Wu F, Cui BK, Yuan Y, Dai YC, Liu XY (2023) Species diversity, updated classify cation and divergence times of the phylum Mucoromycota. Fungal Diversity 123: 49–157.

Zhao H, Wu F, Dai YC, Vlasak J, Ghobad-Nejhad M, Liu HG, Yuan Y (2025) Divergence time and biogeography of the fungal genus *Porodaedalea* (Basidiomycota, Hymenochaetales), obligate phytopathogens on coniferous trees. Molecular Phylogenetics and Evolution 212: 108425. https://doi.org/10.1016/j.ympev.2025.108425